Data report: paleomagnetic and rock magnetic measurements on Hole U1301B basaltic samples[1]

William W. Sager,[2] Bernard A. Housen,[3] and Lisa M. Linville[3]

Chapter contents

[1] Sager, W.W., Housen, B.A., and Linville, L.M., 2008. Data report: paleomagnetic and rock magnetic measurements on Hole U1301B basaltic samples. *In* Fisher, A.T., Urabe, T., Klaus, A., and the Expedition 301 Scientists, *Proc. IODP,* 301: College Station, TX (Integrated Ocean Drilling Program Management International, Inc.). doi:10.2204/iodp.proc.301.204.2009

[2] Department of Oceanography, Texas A&M University, College Station TX 77843, USA.
wsager@tamu.edu

[3] Geology Department, Western Washington University, Bellingham WA 98225, USA.

Abstract

During Integrated Ocean Drilling Program Expedition 301, 235 m of upper igneous crust was cored in Hole U1301B, in an area of hydrothermal circulation on Juan de Fuca Ridge, providing an opportunity to better understand ocean crust magnetization. We studied the paleomagnetism of this section using a variety of techniques. Natural remanent magnetization (NRM) and alternating-field or thermal demagnetization measurements were made on 330 individual samples of igneous rock from both the working-half and archive-half cores. Rock magnetic characterization measurements were made on a subset of samples to better understand the source of the magnetization. These measurements included hysteresis parameters, Curie temperature, and isothermal remanent magnetization (IRM) acquisition. In addition, thin sections were examined for several samples in an effort to visually identify magnetic grains. Igneous samples from Hole U1301B display a range of NRM values between 1.3 and 73.0 A/m with a median value of 6.9 A/m, which are values typical of ocean crust basalts. IRM acquisition curves are consistent with titanomagnetite as the magnetic remanence carrier. Hysteresis parameters indicate single domain and pseudosingle domain behavior, despite large grain sizes seen in scanning electron microphotographs. The apparent paradox is resolved by observation of grain textures that indicate that large grains are split into small domains. Magnetization direction characteristics vary and have been divided into five types by demagnetization patterns. The many patterns suggest that the remanent magnetization of some samples has been altered by secondary processes, such as hydrothermal metamorphism.

Introduction

During Integrated Ocean Drilling Program (IODP) Expedition 301, 3.5 Ma age crust was drilled on the flank of the Juan de Fuca Ridge at Site U1301, located at 47°45.2′N, 127°45.8′W (see the **"Expedition 301 summary"** chapter). The site targeted an area of hydrothermal fluid flow for an experiment examining the hydrology of the ocean crust. Although the ridge flank is buried by unusually thick sediments because of the proximity of land, it is otherwise the site of normal oceanic crust. More than 200 m of upper oceanic crust basalt was cored in Hole U1301B, making it

doi:10.2204/iodp.proc.301.204.2009

one of the relatively few sites where such a large section of crustal rock has been sampled. For scientists who study paleomagnetism, this represents an excellent opportunity to learn more about the magnetization of the upper crust.

We sampled the basalt section from Hole U1301B with the goal of learning about the magnetization properties of the recovered basalt samples. Because the crust appears normal, we expected to find that the basalts were magnetized in the direction of the magnetic field 3.5 m.y. ago, when the crust at Site U1301 was formed. Our working hypothesis was that the samples should behave as typical ocean crust basalts, should be normally polarized (because the site is on a normal polarity magnetic anomaly), and should give magnetization inclinations that are similar to the geocentric axial dipole inclination for the site (65.6°). We also expected that some of the samples would display evidence of hydrothermal alteration, owing to the location of the site in an area of hydrothermal circulation.

Background

Hole U1301B was one of four holes drilled at Site U1301. The drill string encountered the seafloor at a depth of 2656 meters below sea level (mbsl) and penetrated to 582.8 meters below seafloor (mbsf). Drilling in Hole U1301B showed that the upper 265.2 m of the section is sedimentary. Thus, the lower 317.6 m of the drilled section penetrated upper crustal igneous rocks.

Because of problems coring the fractured upper part of the igneous section at nearby Site 1026 during Ocean Drilling Program (ODP) Leg 168 (Shipboard Scientific Party, 1997), the upper 85 m of the igneous section in Hole U1301B was not cored. Only ~5% recovery was obtained throughout this section during Leg 168, so the upper igneous section is not well known. After casing for hole stability during Expedition 301, igneous rocks below 85 m beneath the sediment/basalt contact were continuously cored. A total of 69.1 m of igneous core was recovered from 235 m of cored section for a recovery percentage of ~30%.

The cored igneous section was divided into eight units defined by changes in lava morphology, rock texture, and grain size (see the **"Site U1301"** chapter). Units 1, 3, 5, 7, and 8 are characterized by pillow basalts, whereas Units 2, 4, and 6 are massive units (Fig. **F20** in the "Site U1301" chapter). The massive units are generally thin (<10 m thick), so most of the igneous section (and samples recovered) consists of pillow basalts.

Pillows from the cores are generally sparsely vesicular and micro- or cryptocrystalline in texture. Massive basalts are similar but have few vesicles. Both types of rock are normal depleted mid-ocean-ridge basalts (MORB) as indicated by geochemical analyses (see the **"Site U1301"** chapter). Alteration in the core samples ranges from slight to moderate (5%–25%), with the slightly altered rocks generally dark gray in appearance. The most unaltered parts of the samples are in flow interiors, and the alteration has proceeded to saponite grade (see the **"Site U1301"** chapter). More intense alteration has proceeded generally along cracks and veins, often forming alteration halos around such features. The halos have varied colors (black, brown, and green) depending on the mix of secondary minerals. Potentially magnetic iron oxyhydroxides were found in ~44% of the veins examined, pyrite was found in ~3%, and goethite was found in one vein.

Methods

Shipboard measurements

During Expedition 301, the igneous section was extensively sampled for paleomagnetic study, with measurements made from a total of 330 discrete samples (Tables **T1, T2**). All measurements were made on discrete samples because the igneous core was too discontinuous to allow for reliable measurements from whole core sections. A total of 172 discrete ~15 cm^3 paleomagnetic samples were taken at an average spacing of ~2/m of recovered core. These samples were acquired using a two-blade saw to produce cubes ~25 mm on a side. In order to obtain a greater number of paleomagnetic data points, three other types of samples were also measured. One was ~15 cm^3 discrete cube samples, similar to the paleomagnetic samples except that they were taken for physical property measurements (23 samples). Another was irregular-sized intact oriented pieces (~50–200 cm^3) of the archive-half core (127 samples). In addition, eight pairs of small irregular-sided pieces, usually <5 cm^3 in volume, were collected to investigate the differences in magnetic properties inside and outside of halo alteration zones.

All but the small irregular samples were measured on the shipboard 2G Enterprises model 760R pass-through cryogenic superconducting quantum interference device (SQUID) magnetometer (see the **"Methods"** chapter). Measurements were made using the usual ODP core reference frame with the x-axis in the upcore direction (see the **"Methods"** chapter). The characteristic remanent magnetization (ChRM)

was isolated using either stepwise alternating-field (AF) or thermal demagnetization. All AF demagnetization steps were run on the 2G Enterprises model 2G600 inline demagnetizer that is a part of the pass-through magnetometer system. Thermal heating was accomplished with a Schoenstedt model TSD-1 magnetically shielded oven.

Because the measurement of physical property samples and archive-half core pieces had to be nondestructive, AF demagnetization was used on these samples. Typically, AF demagnetization was done in 5 mT steps from 10 to 40 mT and in 10 mT steps for higher fields. In contrast, most of the samples acquired for paleomagnetic study were thermally demagnetized (see Table **T1**). Most thermal demagnetization analyses used 50°C steps from 150° to 550°C; however, other temperatures were used in some instances to explore magnetization properties.

AF and thermal demagnetization data were plotted for each sample on an orthogonal vector diagram (Zijderfeld, 1967) to aid in interpreting magnetization components and directions. ChRM is assumed to be shown by a section of high-temperature or high-AF field univectorial decay observed on the orthogonal vector plot. Magnetization directions were calculated using principal component analysis (Kirschvink, 1980) from that section of univectorial decay. With only a few exceptions, all of the magnetization directions were determined from calculations that were not anchored to the orthogonal vector plot origin. Typically four to six measurements were used for the principal component analysis. For two samples, the principal component analysis was constrained by only two measurements, so these calculations were anchored to the origin.

Shore-based measurements

Shore-based measurements were made in the paleomagnetic laboratory at Western Washington University with the intent of better understanding the source and characteristics of the magnetization in Hole U1301B basalts. Measurements of Curie temperature and magnetic hysteresis parameters were made on 32 discrete ~15 cm^3 cube samples (Table **T2**). Magnetization direction studies were carried out on these and four additional cube samples. In addition, magnetic hysteresis and isothermal remanent magnetization (IRM) acquisition measurements were conducted on eight pairs of samples in which the two samples of each pair come from an alteration halo and the adjacent slightly altered rock (Tables **T3, T4**).

All samples were treated to detailed AF or thermal demagnetization routines, with all but 4 of the 36 samples being thermally demagnetized. AF demagnetization was carried out in a D-Tech D2000 AF demagnetizer. Compared with previous shipboard analysis, demagnetization steps were more closely spaced at low field values (2–3 mT steps to 10 mT), the same 5 mT steps were used from 10 to 100 mT, and 20 mT steps were used to 200 mT. Thermal demagnetization was also generally more detailed than shipboard analyses, with steps of 10°–20°C being commonly used. Thermal demagnetization was carried out to 450°–580°C, depending on results from any particular sample. Heating was done in an argon-filled environment to prevent oxidation from occurring at high temperatures. Magnetization direction analysis for each of these samples was carried out in the same manner as for the shipboard samples.

Hysteresis loops were measured using a MicroMag vibrating sample magnetometer (VSM) at room temperature in fields of up to 10 kOe. Hysteresis loops before and after heating were also taken for samples for which Curie temperatures were measured in the presence of a magnetic field. Paramagnetic contributions to the hysteresis curves were minimized in most cases by a slope correction using MicroMag software. IRM and backfield curves were also determined with the VSM.

To determine Curie temperature, magnetic susceptibility was measured as a function of temperature using a Kappabridge magnetic susceptibility meter with a furnace attachment. Chips from each sample were powdered and cycled from room temperature to 700°C and back to 40°C in the presence of argon gas to minimize oxidation. Chips from two representative samples were then cut and powdered for closer examination. These samples were run in the same manner as previously described but to a maximum temperature of 320°C. Curie temperatures were determined by the intersecting tangents method from graphs of magnetic susceptibility versus temperature. To gauge the accuracy of susceptibility-based measurements, four paired samples were selected for direct Curie temperature measurement with a furnace-equipped VSM. Curie temperatures for these samples were determined by the second derivative method outlined by Tauxe (1998). Thin sections from these sample pairs were also made, polished, and coated in carbon for scanning electron microscope (SEM) examination.

Results

NRM and directional measurements

Sample natural remanent magnetization (NRM) and directional measurements are given in Table **T1.** NRM values range from 1.3 to 73.0 A/m with a me-

dian value of 6.9 A/m. Most samples have NRM values <10 A/m, and only seven have NRM values >50 A/m (Fig. F1). These values are typical of submarine basalts, and the skewed distribution with a small number of large NRM values is also commonly observed (Johnson and Pariso, 1993; Johnson et al., 1996; Zhao et al., 2006). High NRM values are scattered more or less evenly throughout the section (Fig. F1).

During demagnetization, Hole U1301B samples show a remarkable variety of behavior and ChRM directions (Figs. F2, F3). Samples gave better results with thermal demagnetization, which is why we used that technique for most of the demagnetization experiments. Some AF-demagnetized samples displayed magnetizations that veered from the origin at high field values (Fig. F2D), implying some sort of spurious magnetization imparted by the demagnetization equipment (e.g., a rotational remanent magnetization or gyroremanent magnetization). Most samples displayed a large, steeply downward NRM direction that is probably indicative of the drill-string overprint that is common among paleomagnetic samples cored onboard the *JOIDES Resolution* (see Fig. F2A, F2C, F2E) (Acton et al., 2002; Fuller et al., 2006). In some low-coercivity samples, this overprint dominated magnetizations to the point that it was difficult to determine the ChRM. In samples from the upper part of the igneous section, both AF and thermal demagnetization revealed a ChRM with a downward-directed (positive) inclination between ~30° and 90° (Figs. F2A, F2C, F2F, F3). This magnetization direction indicates normal polarity in the Northern Hemisphere. Some samples give a reversed polarity inclination (i.e., negative or upward). Typically, this ChRM is found at high-temperature steps and is masked by a drill string overprint or a lower temperature normal component similar in dip to the normal ChRM samples (Fig. F2E). A few samples, such as 301-U1301B-6R-2, 35 cm (Fig. F2B), are reversed with no evidence of a downward overprint, and such samples may have been inverted during handling.

To examine ChRM trends, we arbitrarily classify ChRM directions into five classes:

- Type 1 has low inclination, reversed ChRM.
- Types 2 and 3 have normal ChRM inclinations, with those of type 2 having values below ~40° and those of Type 3 having higher values.
- Type 4 is characterized by a dominant drill string overprint (typically low-coercivity samples).
- Type 5 is has two components, a high-temperature reversed inclination and a lower temperature normal direction.

Most samples are Types 2 or 3 (Table T1), especially in the upper part of the section. In the lower part of the section, below 470 mbsf, Types 2 and 3 are still common, but all of the different types are represented with little apparent correlation between adjacent or nearby samples. This part of the section also displays ChRM inclinations with highly scattered values, including negative (apparently reversed) inclinations (Fig. F3).

Because Site U1301 is on a normal polarity magnetic anomaly, we have interpreted the normal inclinations as "normal" and the reversed inclinations as spurious (see the **"Site U1301"** chapter). Even in the apparently normal-behaving upper section, normal polarity inclinations do not precisely match the expected inclination. The average inclination for the section above 470 mbsf is 53.5°, which is less than the geocentric axial dipole inclination for the site of 66.5°. Even if this value is corrected for the slight shallowing caused by averaging azimuthally unoriented samples (corrected expected inclination = 64.2° using Cox and Gordon, 1984) the difference is >10°.

Rock magnetic measurements

IRM acquisition curves all saturate quickly in low (<100 mT) applied fields (Fig. F4; Table T2). This low-field IRM saturation is characteristic of titanomagnetite grains. The flat high-field sections of the curves indicate the absence of high-coercivity magnetic minerals, such as hematite. Observed differences between samples from alteration halos and nearby samples from slightly altered core are small but systematic. Samples from alteration halos consistently require slightly greater applied fields to reach saturation (Fig. F4), implying that the alteration slightly raises the coercivity of the bulk assemblage of magnetic grains.

Thermomagnetic curves for Hole U1301B basalt samples are usually nonreversible, although some samples do give reversible curves (Fig. F5). Nonreversibility implies changes in the magnetic mineral assemblage caused by heating. In these samples, we are probably seeing the conversion of maghemite into other magnetic minerals. The thermomagnetic curves give Curie temperatures for Hole U1301B samples ranging from 128° to 370°C (Tables T3, T4) with a median value of 339°C. Most samples give values in the 240°–320°C range. These values are typical for altered ocean basalts with titanomagnetite magnetic grains.

Magnetic hysteresis data (Tables T3, T4) show that all samples have saturation remanence/saturation magnetization (M_r/M_s) ratios <0.5 and remanent co-

ercive force/ordinary coercive force (H_{cr}/H_c) ratios of <5. Most samples plot near the single domain (SD) field on the Day plot (Fig. F6), although some samples have hysteresis parameter ratios that fall in the pseudosingle domain (PSD) region. Of the paired samples from alteration halos and nearby slightly altered rock, it appears that the more altered samples plot preferentially toward the SD region of the plot, suggesting that the alteration process makes magnetic grains behave more like SD grains. Most samples plot near model lines (Dunlop, 2002) for mixtures of SD and multidomain (MD) grains. Given microscopic observations (see below) that indicate both large and small magnetic grains, these samples may indeed be displaying the behavior of a SD/MD grain mixture.

On a Day plot, samples with different demagnetization behaviors show no indication of clustering (Fig. F7). Samples with each different demagnetization behavior are found scattered throughout the hysteresis ratio range of the entire sample population. This implies that different types of demagnetization behavior are not a function of magnetic grain size.

SEM photomicrographs (Fig. F8) show that large titanomagnetite grains are found in sample thin sections. These grains are often rectangular or deltoid in appearance, which is typical of titanomagnetite. Many of these grains are tens of micrometers in diameter, which is far larger than the normal size for SD or PSD grains. Indeed, grains of this size should behave as multidomain grains. An explanation for the difference is that many of the grains show trellis, dendritic, skeletal, and cruciform patterns within the grains, indicating that the grains are broken up internally into smaller pieces. Furthermore, the surfaces of these grains are often invaded by cracks, implying further divisions. In sum, the naturally occurring fractures and crystal structures tend to be much smaller than the whole grain. In addition, electron dispersive scattering (EDS) tests imply that titanomagnetites are also found within the groundmass, so there is likely to be a very small size grain component also existing within these samples.

Acknowledgments

This research used samples and data provided by the Integrated Ocean Drilling Program (IODP). IODP is sponsored by the U.S. National Science Foundation (NSF) and participating countries under management of Joint Oceanographic Institutions (JOI), Inc. (renamed The Consortium for Ocean Leadership). W. Sager was supported for this research by a grant from the JOI/U.S. Science Support Program. L. Linville was supported with a supplement to that grant for undergraduate education. B. Housen acknowledges support from NSF grants EAR-MRI-0421457 for the vibrating sample magnetometer and EAR-IR-9727032 for the cryogenic magnetometer in the laboratory at Western Washington University.

References

Acton, G.D., Okada, M., Clement, B.M., Lund, S.P., and Williams, T., 2002. Paleomagnetic overprints in ocean sediment cores and their relationship to shear deformation caused by piston coring. *J. Geophys. Res.,* 107(B4):2067. **doi:10.1029/2001JB000518**

Cox, A., and Gordon, R.G., 1984. Paleolatitudes determined from paleomagnetic data from vertical cores. *Rev. Geophys. Space Phys.,* 22(1):47–71. **doi:10.1029/RG022i001p00047**

Dunlop, D.J., 2002. Theory and application of the Day plot (M_{rs}/M_s versus H_{cr}/H_c), 1. Theoretical curves and tests using titanomagnetite data. *J. Geophys. Res.,* 107(B3):2056. **doi:10.1029/2001JB000486**

Fuller, M., Molina-Garza, R., Touchard, Y., and Kidane, T., 2006. Paleomagnetic records from carbonate legs in the Southern Oceans and attendant drilling and coring related effects. *In* Sager, W.W., Acton, G.D., Clement, B.M., and Fuller, M. (Eds.), *ODP Contributions to Paleomagnetism.* Phys. Earth Planet. Int., 156(3–4):242–260. **doi:10.1016/j.pepi.2005.08.007**

Johnson, H.P., and Pariso, J.E., 1993. Variations in oceanic crustal magnetization: systematic changes in the last 160 million years. *J. Geophys. Res.,* 98(B1):435–445. **doi:10.1029/92JB01322**

Johnson, H.P., Van Patten, D.V., and Sager, W.W., 1996. Age-dependent variation in the magnetization of seamounts. *J. Geophys. Res.,* 101(B6):13701–13714. **doi:10.1029/96JB00537**

Kirschvink, J.L., 1980. The least-squares line and plane and the analysis of palaeomagnetic data. *Geophys. J. R. Astron. Soc.,* 62(3):699–718.

Shipboard Scientific Party, 1997. Rough basement transect (Sites 1026 and 1027). *In* Davis, E.E., Fisher, A.T., Firth, J.V., et al., *Proc. ODP, Init. Repts.,* 168: College Station, TX (Ocean Drilling Program), 101–160. **doi:10.2973/odp.proc.ir.168.105.1997**

Tauxe, L., 1998. *Paleomagnetic Principles and Practice:* Dordrecht, Netherlands (Kluwer Academic Publishers.

Zhao, X., Riisager, P., Antretter, M., Carlut, J., Lippert, P., Liu, Q., Galbrun, B., Hall, S., Delius, H., and Kanamatsu, T., 2006. Unraveling the magnetic carriers of igneous cores from the Atlantic, Pacific, and the southern Indian oceans with rock magnetic characterization. *In* Sager, W.W., Acton, G.D., Clement, B.M., and Fuller, M. (Eds.), *ODP Contributions to Paleomagnetism.* Phys. Earth Planet. Int., 156(3–4):294–328. **doi:10.1016/j.pepi.2005.08.005**

Zijderveld, J.D.A., 1967. AC demagnetization of rocks: analysis of results. *In* Collinson, D.W., Creer, K.M., and Runcorn, S.K. (Eds.), *Methods in Palaeomagnetism:* New York (Elsevier), 254–286.

Initial receipt: 29 May 2007
Acceptance: 18 February 2008
Publication: 7 April 2009
MS 301-204

Figure F1. Natural remanent magnetization (NRM) of basalt samples, Hole U1301B.

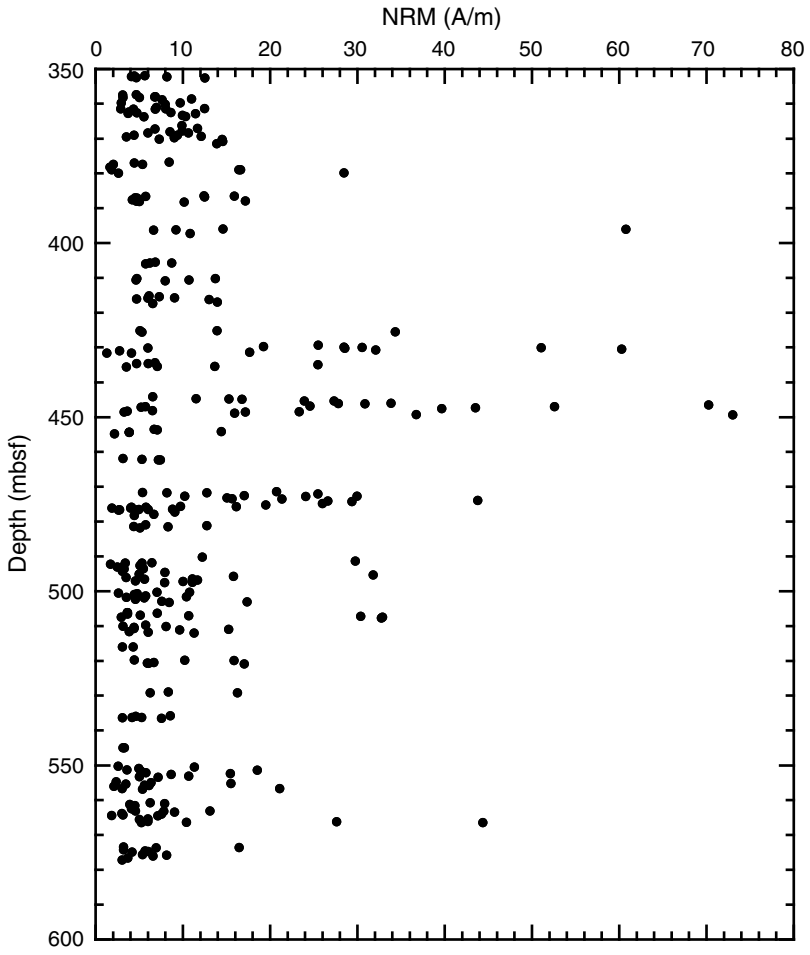

Figure F2. Basalt sample demagnetization behavior, Hole U1301B. **A–D.** Alternating-field demagnetization. (A) Sample 301-U1301B-30R-1, 98 cm, has a positive inclination, indicating normal polarity at the drill site. (B) Although Sample 301-U1301B-6R-2, 35 cm, would normally be considered to have a reversed magnetization (i.e., negative inclination), the sample gives an isolated result and shows no downward overprint, as do most other samples, so it is thought to have been accidentally inverted during curation. (C) Sample 301-U1301B-32R-1, 36 cm, shows a large downward drill string overprint. (D) Sample 301-U1301B-3R-1, 110 cm, veers from the simple univectorial decay at high-field demagnetization steps. **E–F.** Thermal demagnetization. (E) Sample 301-U1301B-30R-1, 99 cm, shows two components with a high-temperature reversed polarity characteristic magnetization, whereas (F) Sample 301-U1301B-5R-2, 109 cm, shows a normal polarity magnetization after removal of the drill string overprint. The latter is an example of Type 2 or 3 behavior. Sample 301-U1301B-30R-1, 99 cm, is an example of Type 5 behavior. If the inclination were shallower, it would be classified as Type 1 (see **"NRM and directional measurements"** for discussion of behavior classes).

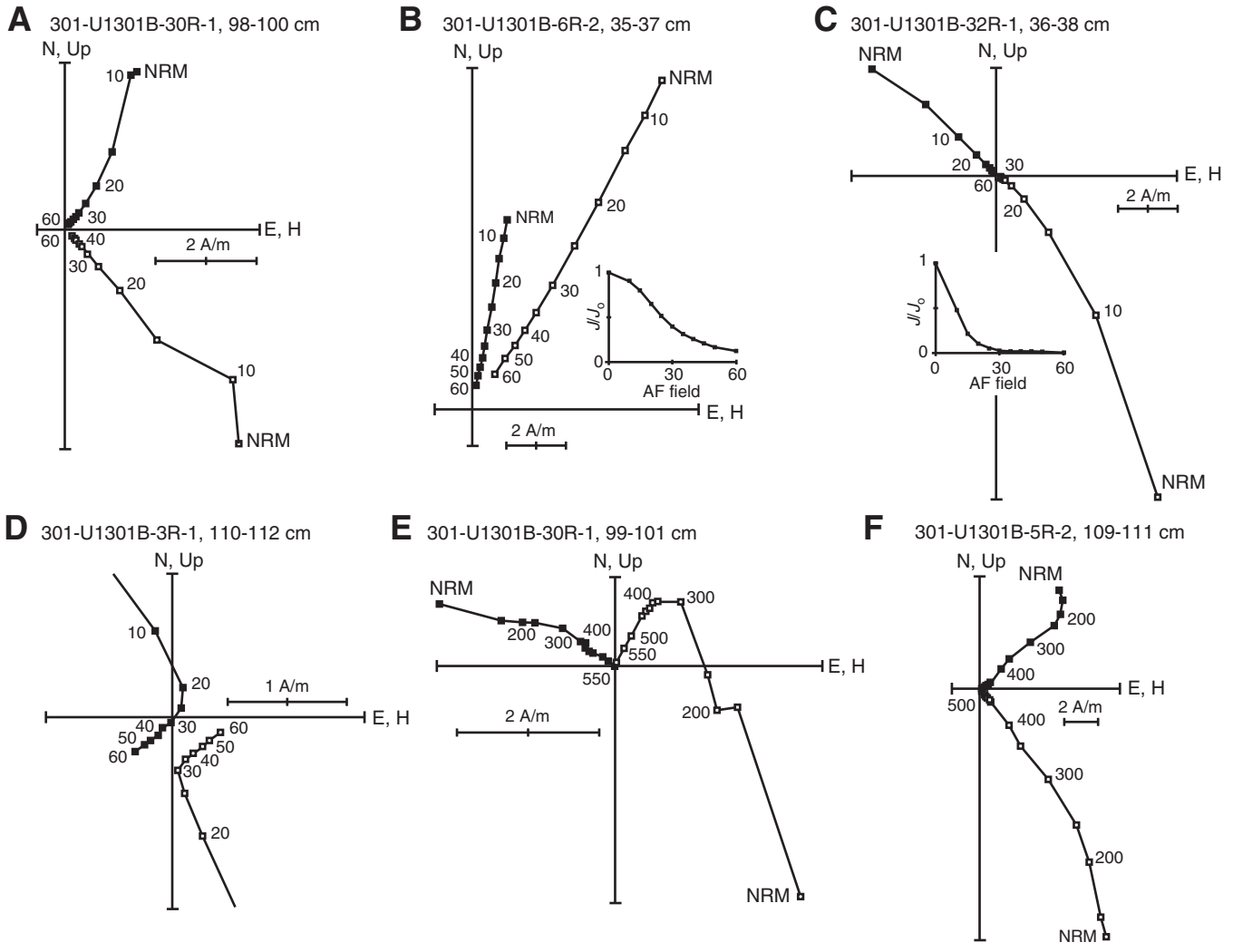

Figure F3. ChRM inclination values for basalt samples, Hole U1301B. Dotted vertical lines show expected geocentric axial dipole inclination for site location.

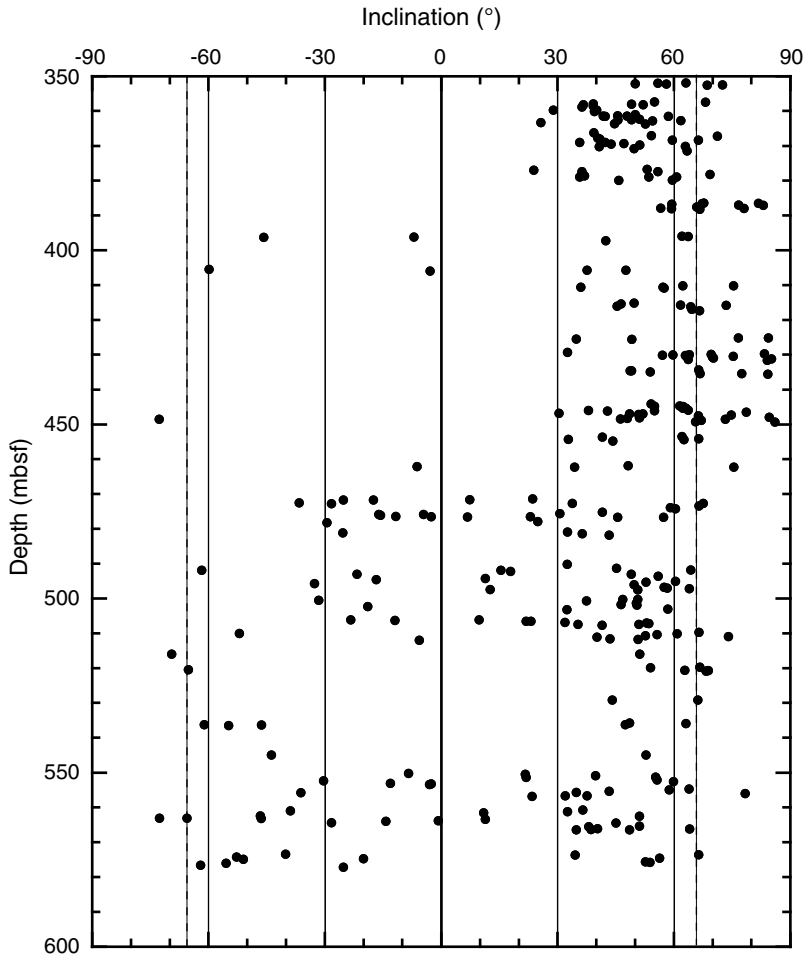

Figure F4. IRM acquisition curve for two representative samples, Hole U1301B. One sample is from relatively unaltered core and the other is from an adjacent alteration halo.

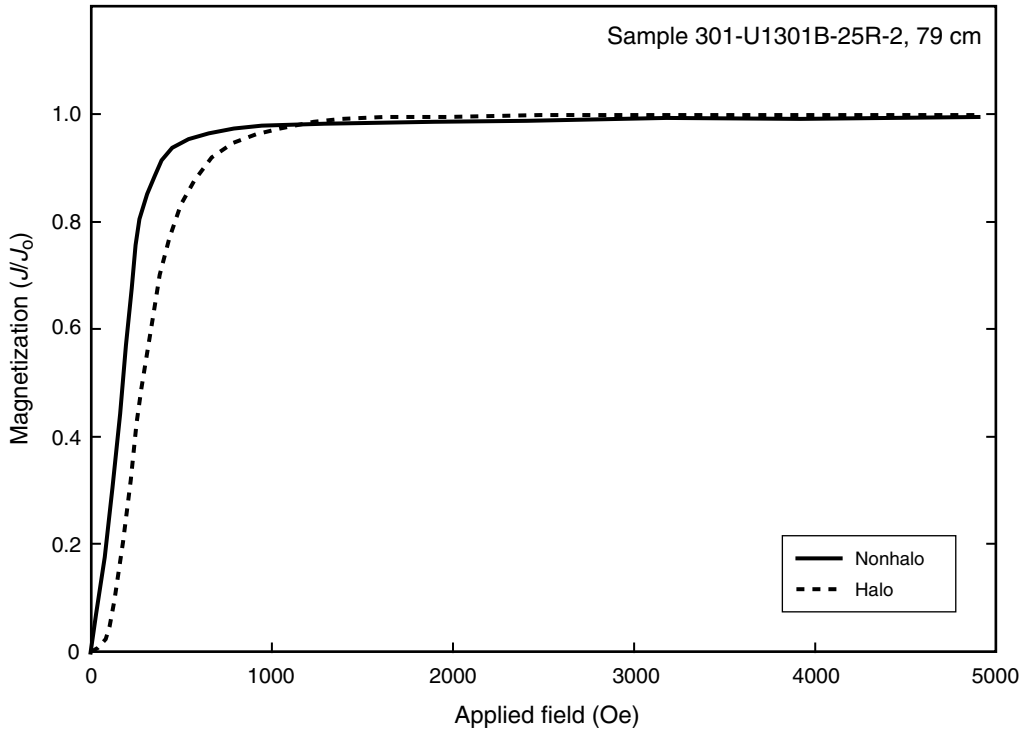

Figure F5. Magnetization behavior upon heating and cooling of two representative basalt samples, Hole U1301B. Sample 301-U1301B-13R-1, 130 cm, shows a reversible curve and gives a Curie temperature (*Tc*) of 179°C. Sample 301-U1301B-20R-1, 28 cm, is not reversible upon cooling and gives a Curie temperature of 339°C.

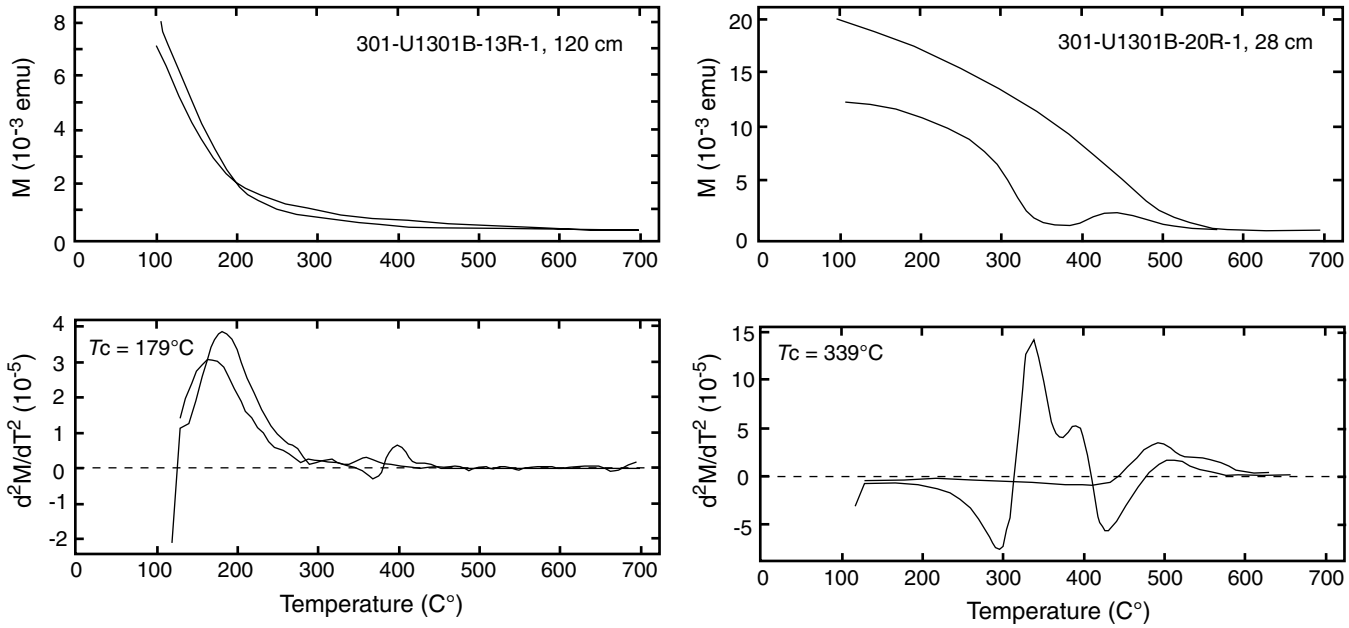

Figure F6. M_r/M_s vs. H_{cr}/H_c Day plot for basalt samples, Hole U1301B. Vertical and horizontal lines define boundaries of different magnetic grain size fields: SD = single domain, PSD = pseudosingle domain, MD = multidomain. Dotted lines show two example mixing lines for combinations of single and multidomain grains (Dunlop, 2002). Plot axes are logarithmic.

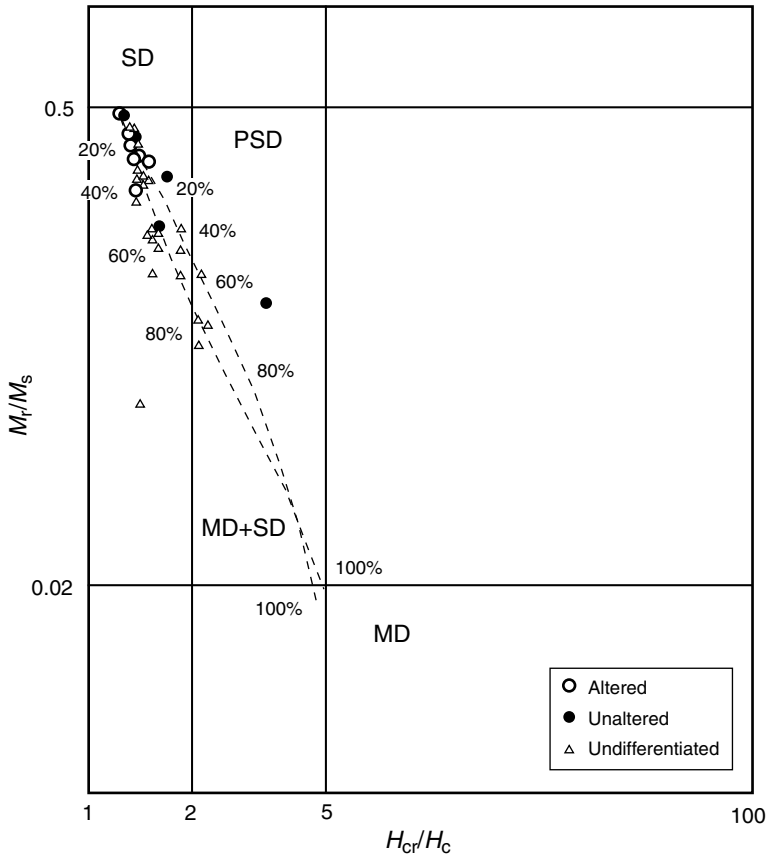

Figure F7. M_r/M_s vs. H_{cr}/H_c Day plot for basalt samples showing different types of demagnetization behaviors, Hole U1301B (see **"NRM and directional measurements"** for explanation). SD = single domain, PSD = pseudosingle domain, MD = multidomain.

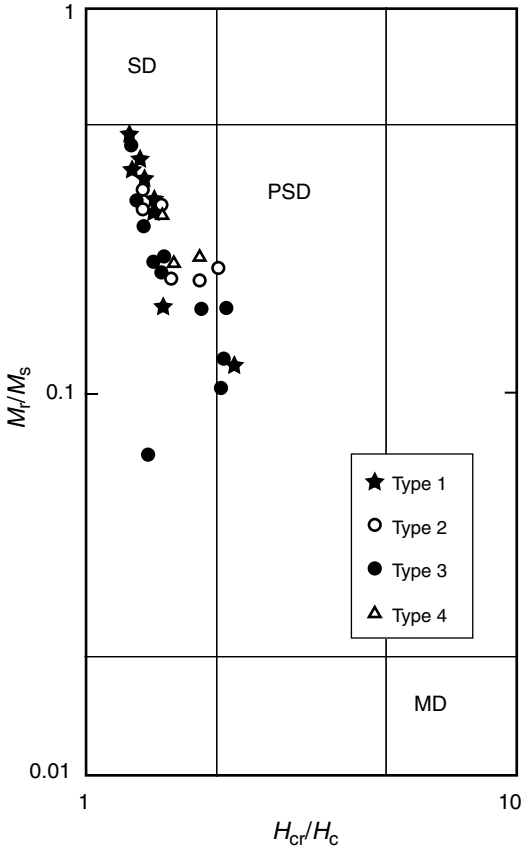

Figure F8. Polished thin section photomicrographs from representative basalt samples, Hole U1301B. Scale bar = 50 µm. **A.** Sample 301-U1301B-18R-1, 36 cm, alteration halo. **B.** Same as A from slightly altered rock. **C.** Sample 301-U1301B-15R-1, 44 cm, slightly altered.

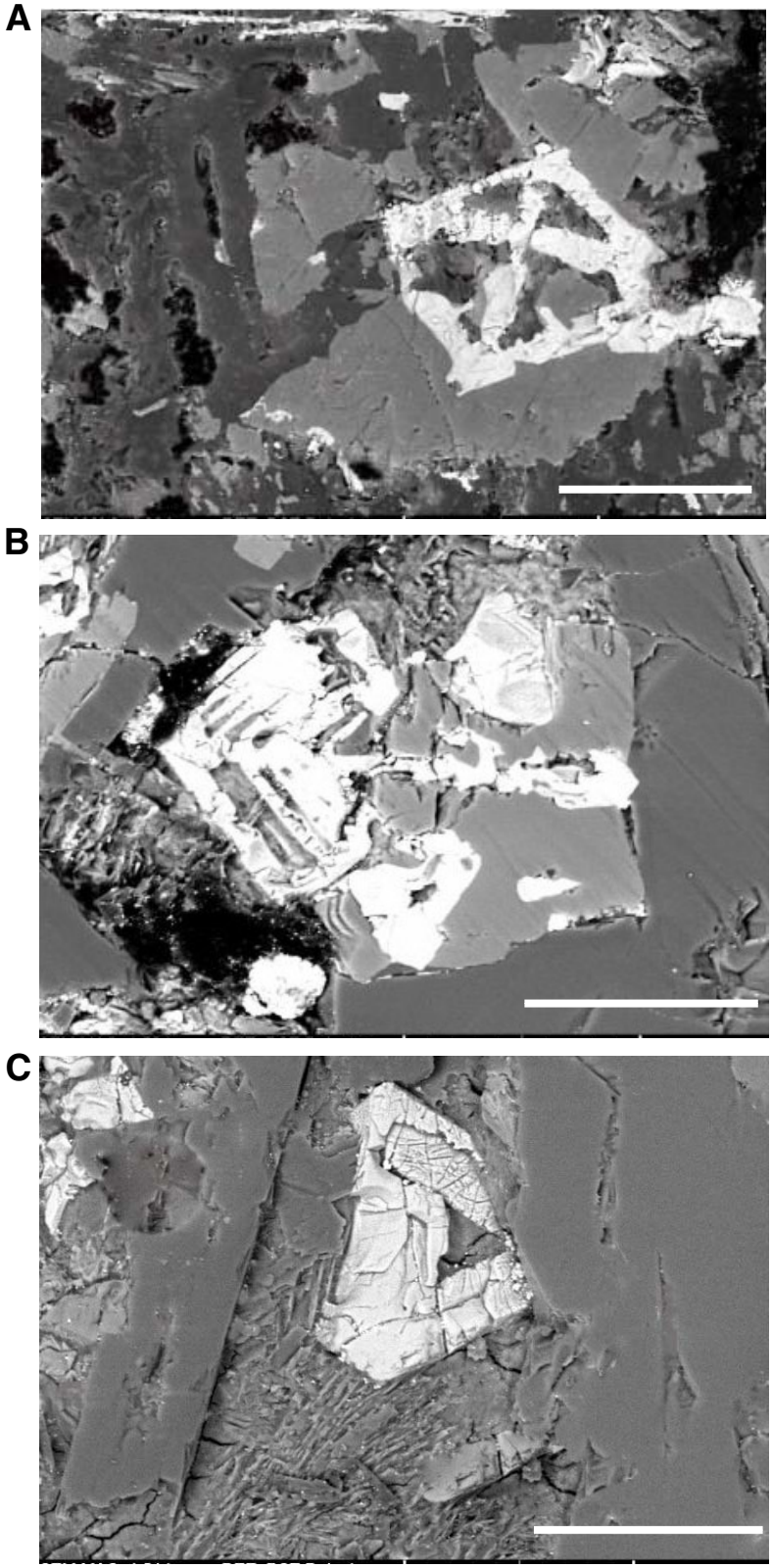

Table T1. Basalt sample paleomagnetic data, Hole U1301B. (See table notes.) (Continued on next four pages.)

Core, section, interval (cm)	Depth (mbsf)	Unit	Unit type	NRM (A/m)	Inc. (°)	*N*	MAD	Sample type	Demagnetization			ChRM type
									Steps	Treatment	Quality	
301-U1301B-												
1R-1, 70	351.88	1B	P	5.71	63.2	5	2.8	AR	15–35	AF	A	3
1R-1, 72	351.90	1B	P	4.51	56.0	5	2.2		300–475	TH	A	3
1R-1, 87	352.07	1B	P	4.16	50.1	4	2.1	AR	25–40	AF	A	3
1R-1, 92	352.10	1B	P	8.22	58.2	5	1.6		300–475	TH	A	3
1R-1, 120	352.40	1B	P	4.71	72.7	4	0.9	AR	15–25	AF	C	3
1R-1, 130	352.50	1B	P	12.59	68.7	7	1.6		20–50	AF	A	3
2R-1, 17	357.27	1C	P	4.72	55.1	6	4.0	AR	25–50	AF	A	3
2R-1, 30	357.40	1C	P	3.16	68.3	5	1.9	AR	30–50	AF	A	3
2R-1, 73	357.83	1C	P	6.90	39.3	5	1.8	PP	20–40	AF	C	2
2R-1, 79	357.89	1C	P	6.81	49.2	5	4.6		300–475	TH	A	2
2R-1, 100	358.10	1C	P	3.18	52.2	4	2.1	AR	35–50	AF	A	3
2R-1, 100	358.10	1C	P	5.07	36.8	6	1.5		400–540	TH	A	2
2R-1, 137	358.47	1C	P	11.06	39.3	8	0.9		20–60	AF	C	2
2R-2, 22	358.76	1C	P	7.68	36.4	7	2.1		20–50	AF	A	2
2R-2, 110	359.64	1C	P	3.00	40.2	5	1.3	AR	30–50	AF	A	2
2R-2, 115	359.69	1C	P	9.75	29.0	6	1.2	PP	15–40	AF	A	2
2R-3, 3	360.07	1C	P	8.05	39.6	4	3.4		25–40	AF	C	2
2R-3, 95	360.99	1C	P	7.02	50.1	7	9.3		350–550	TH	A	3
2R-3, 123	361.27	1C	P	12.57	45.6	6	1.0	PP	20–50	AF	A	2
3R-3, 130	361.34	1C	P	2.95	41.9	5	1.7	AR	30–50	AF	A	2
3R-1, 24	361.34	1C	P	8.09	48.0	3	4.9		300–450	TH	A	3
3R-1, 30	361.40	1C	P	4.41	58.7	5	1.4	AR	20–40	AF	A	3
3R-1, 31	361.41	1C	P	6.90	42.4	6	0.4	PP	15–40	AF	A	2
3R-1, 112	362.22	1C	P	3.88	51.2	6	0.7	AR	25–50	AF	A	3
3R-1, 130	362.40	1C	P	8.70	49.2	5	0.7		15–35	AF	B	3
3R-1, 135	362.45	1C	P	4.80	45.7	6	0.9	AR	25–50	AF	A	2
3R-2, 10	362.68	1C	P	3.79	61.9	5	1.9	AR	30–50	AF	A	3
3R-2, 12	362.70	1C	P	11.49	–54.6*	5	0.5		250–450	TH	A	3
3R-2, 58	363.18	1C	P	10.00	25.8	6	0.5	PP	20–50	AF	A	2
3R-2, 88	363.48	1C	P	10.37	44.8	5	0.4		20–40	AF	A	2
3R-2, 107	363.67	1C	P	5.60	52.8	5	0.5	AR	30–50	AF	A	3
4R-1, 37	366.97	1C	P	11.74	54.3	4	0.1		250–450	TH	A	3
4R-1, 51	366.11	1C	P	9.96	39.5	5	1.4		420–540	TH	A	2
4R-1, 55	367.15	1C	P	6.88	71.3	4	0.8	AR	35–50	AF	C	3
4R-1, 110	367.70	1C	P	9.98	40.5	5	1.3	PP	25–45	AF	A	2
4R-1, 134	367.94	1C	P	8.59	41.0	4	10.0		350–500	TH	A	2
4R-2, 20	368.26	1C	P	6.06	59.7	4	2.0	AR	40–60	AF	C	3
4R-2, 23	368.29	1C	P	10.70	66.4	4	1.1		20–35	AF	A	3
4R-2, 84	368.90	1C	P	4.45	42.4	5	0.6	AR	30–50	AF	A	2
4R-2, 88	368.94	1C	P	9.41	35.8	5	1.8		250–500	TH	A	2
4R-3, 1	369.40	1C	P	3.58	43.9	5	1.5	AR	35–60	AF	A	2
4R-3, 25	369.24	1C	P	12.18	47.2	4	2.2		300–500	TH	A	2
4R-3, 27	369.66	1C	P	9.07	51.3	6	2.8		25–60	AF	A	3
4R-3, 64	370.03	1C	P	7.33	63.1	5	2.2	AR	30–50	AF	B	3
4R-3, 78	370.17	1C	P	14.55	40.9	5	1.1		25–45	AF	B	2
4R-3, 132	370.71	1C	P	14.61	49.9	5	1.7	PP	20–40	AF	A	2
4R-4, 45	371.29	1C	P	13.94	63.5	4	1.1		200–400	TH	B	3
5R-1, 37	376.67	1C	P	8.48	53.2	6	1.4		25–60	AF	A	3
5R-1, 57	376.87	1C	P	4.47	24.0	4	0.5	AR	40–60	AF	A	2
5R-1, 100	377.30	1C	P	2.08	56.0	5	2.7	AR	35–60	AF	A	3
5R-1, 100	377.30	1C	P	5.45	36.4	6	0.6		350–520	TH	A	2
5R-2, 27	378.07	1C	P	1.69	69.4	5	0.5	AR	30–50	AF	A	3
5R-2, 104	378.84	1C	P	16.65	35.8	6	3.5	PP	30–50	AF	A	2
5R-2, 105	378.85	1C	P	1.92	60.8	5	2.0	AR	35–60	AF	A	3
5R-2, 109	378.89	1C	P	16.49	53.6	7	1.9		275–475	TH	B	3
5R-3, 44	379.74	1C	P	28.52	59.7	4	12.6		375–475	TH	A	3
5R-3, 55	379.85	1C	P	2.69	45.9	5	1.6	AR	35–60	AF	A	2
6R-1, 33	386.33	1C	P	12.49	67.8	5	2.7		150–350	TH	B	3
6R-1, 41	386.41	1C	P	15.96	81.9	4	1.5	PP	25–40	AF	C	3
6R-1, 48	386.48	1C	P	5.78	67.4	3	1.6	AR	45–60	AF	B	3
6R-1, 64	386.64	1C	P	12.53	59.6	4	2.4		35–60	AF	B	3
6R-1, 86	386.86	1C	P	4.59	76.8	4	1.5	AR	30–45	AF	B	4
6R-1, 92	386.92	1C	P	4.81	83.2	6	1.7	AR	30–60	AF	B	4
6R-2, 4	387.49	1C	P	4.28	66.0	5	3.3	AR	35–60	AF	A	3
6R-2, 35	387.80	1C	P	17.24	–56.7*	5	0.4	PP	35–60	AF	A	3
6R-2, 44	387.89	1C	P	4.74	78.2	5	2.5	AR	35–60	AF	A	3
6R-2, 48	387.93	1C	P	5.07	59.5	5	4.6		420–540	TH	A	3

Table T1 (continued). (Continued on next page.)

Core, section, interval (cm)	Depth (mbsf)	Unit	Unit type	NRM (A/m)	Inc. (°)	*N*	MAD	Sample type	Demagnetization			ChRM type
									Steps	Treatment	Quality	
6R-2, 67	388.12	1C	P	10.22	66.8	4	1.2		350–475	TH	A	3
7R-1, 29	395.89	1C	P	14.67	62.2	6	0.9		25–60	AF	C	3
7R-1, 30	395.90	1C	P	60.81	63.8	6	1.6	AR	30–60	AF	A	3
7R-1, 52	396.12	1C	P	9.26	–6.9	4	1.7		150–275	TH	A	1
7R-1, 57	396.17	1C	P	6.68	–45.6	4	3.5	AR	35–50	AF	A	1
7R-2, 4	397.14	1C	P	10.90	42.6	4	12.8	PP	40–60	AF	C	2
8R-1, 19	405.39	1C	P	6.90	–59.7	5	1.8		35–60	AF	B	1
8R-1, 43	405.63	1C	P	6.26	37.7	6	0.3	AR	30–60	AF	A	2
8R-1, 44	405.64	1C	P	8.79	47.7	6	1.0		30–60	AF	A	2
8R-1, 63	405.83	1C	P	5.78	–2.8	3	1.9	AR	45–60	AF	C	1
9R-1, 30	410.50	1C	P	10.76	57.3	4	10.3		425–500	TH	A	3
9R-1, 32	410.52	1C	P	4.69	36.1	4	2.9	AR	40–60	AF	A	2
9R-1, 53	410.73	1C	P	8.03	57.6	5	0.4	AR	35–60	AF	A	3
9R-1, 63	410.03	1C	P	13.78	75.5	5	7.9		400–500	TH	A	4
9R-1, 63	410.03	1C	P	4.79	62.4	4	0.8	AR	30–45	AF	A	3
10R-1, 26	415.06	1C	P	6.18	49.8	5	0.7	AR	35–60	AF	A	2
10R-1, 45	415.25	1C	P	7.37	46.5	3	2.0		30–40	AF	C	2
10R-1, 79	415.59	1C	P	9.11	61.8	5	8.7		400–500	TH	A	3
10R-1, 95	415.75	1C	P	6.05	73.6	5	5.7		400–500	TH	A	3
10R-1, 131	416.11	1C	P	13.04	64.5	6	4.5		375–500	TH	A	3
10R-2, 57	416.82	1C	P	14.02	64.8	4	1.5		35–50	AF	A	3
10R-2, 67	415.92	1C	P	4.73	45.5	5	1.1	AR	35–60	AF	C	2
10R-2, 96	417.21	1C	P	6.62	66.7	4	2.4	AR	40–60	AF	C	4
11R-1, 67	425.07	2A	M	5.14	76.7	4	1.2	AR	40–60	AF	A	4
11R-1, 68	425.08	2A	M	13.96	84.5	4	3.4		425–500	TH	B	4
11R-1, 94	425.34	2A	M	34.41	35.0	3	6.3		450–500	TH	A	2
11R-1, 107	425.47	2A	M	5.36	49.3	5	1.5	AR	30–45	AF	B	2
12R-1, 27	429.17	2A	M	25.58	32.7	6	8.8		300–500	TH	A	2
12R-1, 70	429.60	2A	M	19.28	83.5	5	2.2		190–235	TH	C	5
12R-1, 91	429.81	2A	M	28.52	69.7	6	3.8		30–60	AF	A	3
12R-1, 93	429.83	2A	M	30.58	64.1	6	2.9		30–60	AF	A	3
12R-1, 100	429.90	2A	M	51.14	59.9	5	2.6		25–45	AF	A	3
13R-1, 14	430.04	2A	M	6.06	57.1	5	2.7	AR	35–60	AF	A	3
13R-1, 22	430.12	2A	M	28.60	63.1	4	12.4		400–475	TH	B	3
13R-1, 45	430.35	2A	M	60.35	75.4	4	3.3		250–300	TH	A	3
13R-1, 68	430.58	2A	M	32.17	70.1	5	6.3		30–50	AF	A	3
13R-1, 94	430.84	2A	M	2.80	70.3	5	1.1	AR	30–50	AF	A	3
13R-1, 120	431.10	2A	M	70.27	85.3	5	5.1		300–420	TH	A	5
13R-2, 5	431.30	2A	M	17.70	63.8	4	13.8		350–450	TH	A	3
13R-2, 14	431.47	2A	M	4.18	84.2	3	0.6	AR	40–50	AF	C	4
13R-2, 17	431.50	2A	M	1.33				AR		AF		
14R-1, 26	434.26	2B	M	6.88	66.5	4	0.4	AR	30–45	AF	B	3
14R-1, 45	434.45	2B	M	4.75	49.2	4	8.7	AR	35–50	AF	C	2
14R-1, 55	434.55	2B	M	6.08	48.8	5	7.2	AR	30–50	AF	A	2
14R-1, 81	434.81	2B	M	25.51	54.0	5	4.8		30–50	AF	A	4
14R-1, 132	435.32	3	P	13.73	77.6	4	1.4		250–375	TH	D	4
14R-1, 133	435.33	3	P	7.13	66.9	3	1.3	AR	45–60	AF	A	3
14R-1, 142	435.42	3	P	3.61	84.3	4	0.7	AR	35–50	AF	B	4
15R-1, 45	444.05	3	P	6.61	54.2	4	1.1	AR	35–50	AF	A	3
15R-1, 94	444.54	4A	M	11.58	61.6	3	5.0		425–500	TH	A	3
15R-1, 108	444.68	4B	M	15.33	55.1	4	12.1	PP	35–50	AF	B	3
15R-1, 113	444.73	4B	M	16.83	62.5	7	1.8		20–50	AF	A	3
15R-2, 9	445.19	4B	M	27.40	63.2	6	5.2		20–45	AF	A	3
15R-2, 20	445.30	4B	M	23.98	62.4	4	8.3	PP	20–35	AF	A	3
15R-2, 70	445.80	4B	M	35.93	63.8	3	5.6		380–460	TH	B	3
15R-2, 78	445.88	4B	M	33.91	38.1	2	3.0		460–515	TH	B[†]	2
15R-2, 91	446.01	4B	M	27.89	55.1	6	14.4		350–475	TH	A	3
15R-2, 93	446.03	4B	M	30.91	43.0	5	4.7		30–50	AF	A	2
15R-2, 127	446.37	4B	M	70.31	78.8	4	1.4		335–420	TH	B	3
15R-3, 10	446.70	4B	M	24.62	30.5	5	3.7		35–60	AF	A	2
15R-3, 22	446.82	4B	M	5.76	48.7	3	1.3	AR	35–45	AF	C	2
15R-3, 24	446.84	4B	M	52.63	52.1	4	3.6		460–540	TH	A	2
15R-3, 41	447.01	4B	M	5.26	51.0	4	0.6	AR	40–60	AF	A	3
15R-3, 63	447.23	4B	M	43.61	74.9	6	7.1		95–180	AF	A	3
15R-3, 81	447.41	4B	M	39.73	66.4	5	1.2		35–60	AF	A	3
15R-3, 120	447.80	4B	M	41.45	84.7	3	1.3		370–450	TH	B	5
15R-3, 144	448.04	4B	M	6.58	51.2	4	1.8	PP	30–45	AF	B	3
15R-4, 5	448.15	4C	M	3.67	48.1	5	0.4	AR	35–60	AF	B	2

Table T1 (continued). (Continued on next page.)

Core, section, interval (cm)	Depth (mbsf)	Unit	Unit type	NRM (A/m)	Inc. (°)	*N*	MAD	Sample type	Demagnetization			ChRM type
									Steps	Treatment	Quality	
15R-4, 21	448.31	4C	M	23.39	46.3	4	9.2		25–40	AF	A	2
15R-4, 29	448.39	4C	M	3.30	–72.6*	4	3.0	AR	35–50	AF	A	4
15R-4, 30	448.40	4C	M	17.24	73.4	4	2.6		370–500	TH	A	3
15R-4, 65	448.75	4C	M	15.99	67.2	5	3.9	PP	20–45	AF	A	3
15R-4, 101	449.11	4C	M	36.80	65.7	4	1.4		40–60	AF	A	3
15R-4, 115	449.25	4C	M	73.04	86.2	4	1.0		350–450	TH	B	5
16R-1, 22	453.42	5	P	6.76	62.2	3	1.3	AR	35–45	AF	B	3
16R-1, 38	453.58	5	P	7.14	41.7	4	2.2	AR	40–60	AF	B	2
16R-1, 81	454.01	5	P	14.46	66.5	4	6.0		425–500	TH	A	3
16R-1, 100	454.20	5	P	3.91	32.9	3	3.4	AR	45–60	AF	A	2
16R-1, 107	454.27	5	P	3.90	62.7	5	2.0		20–40	AF	B	3
16R-1, 144	454.64	5	P	2.23	44.4	4	7.5	PP	30–45	AF	C	2
17R-1, 32	461.72	5	P	3.19	48.3	5	8.9		400–500	TH	A	2
17R-1, 58	461.98	5	P	5.36	–6.1	4	2.0	AR	40–60	AF	A	1
17R-1, 73	462.13	5	P	7.47	75.6	4	19.3	PP	30–45	AF	B	4
17R-1, 76	462.16	5	P	7.26	34.5	6	5.9		375–500	TH	A	2
18R-1, 34	471.34	6	M	20.80	23.7	5	11.9		400–500	TH	A	2
18R-1, 53	471.53	6	M	5.43	7.5	4	3.5	AR	30–50	AF	C	2
18R-1, 55	471.55	6	M	8.23	–17.4	3	5.0		460–540	TH	A	5
18R-1, 65	471.65	6	M	12.83	–25.1	4	2.0		425–500	TH	A	1
18R-1, 96	471.96	6	M	25.51				PP		AF	D	
18R-2, 13	472.43	6	M	17.07	–36.5	5	1.6	PP	20–40	AF	A	1
18R-2, 24	472.54	6	M	10.28	33.9	4	6.6	AR	35–50	AF	B	2
18R-2, 32	472.62	6	M	30.02	67.7	3	7.1		45–60	AF	D	1
18R-2, 50	472.70	6	M	24.14	–28.2	2	4.3		420–460	TH	B†	5
18R-2, 78	473.08	6	M	15.11				PP		AF	D	
18R-2, 102	473.32	6	M	15.69	66.60	6	10.4		300–450	TH	C	3
18R-2, 108	473.38	6	M	21.42						AF	D	
18R-3, 25	473.81	6		43.83	59.20	5	4.3		300–420	TH	B	3
18R-3, 44	474.00	6	M	26.67						TH	D	
18R-3, 58	474.14	6	M	29.42	60.50	3	8.1		500–540	TH	B	3
18R-3, 112	474.68	6	M	26.04						AF	D	
18R-4, 21	475.09	6	M	19.57	41.7	3	3.2		475–525	TH	A	2
18R-4, 65	475.53	6	M	9.78	30.7	4	7.9	AR	30–45	AF	C	2
18R-4, 71	475.59	6	M	16.16				PP		AF	D	
18R-4, 84	475.72	6	M	4.18	–4.4	3	7.2		450–500	TH	C	5
18R-4, 84	475.72	6	M	5.83	–16.0	3	10.5	AR	40–60	AF	A	1
18R-4, 112	476.00	7A	P	1.93	–15.5	5	4.5		420–540	TH	A	5
18R-4, 115	476.03	7A	P	4.06				PP		AF	D	
18R-5, 5	476.38	7A	P	6.08	23.1	5	5.4		35–60	AF	B	2
19R-1, 21	476.31	7A	P	8.88	–11.6	5	0.5	AR	35–60	AF	A	1
19R-1, 32	476.42	7A	P	4.99	–2.5	4	6.8		40–60	AF	B	5
19R-1, 35	476.45	7A	P	2.78	6.9	3	2.7		450–500	TH	A	2
19R-1, 47	476.57	7A	P	4.80	45.6	3	0.2	AR	30–40	AF	B	2
19R-1, 51	476.61	7A	P	2.67	57.5	4	1.9		25–40	AF	B	3
19R-1, 105	477.15	7A	P	9.12						AF	D	
19R-2, 28	477.85	7A	P	6.75	25.0	4	15.6		400–475	TH	A	2
19R-2, 58	478.15	7A	P	4.49	–29.3	3	0.5	AR	35–45	AF	C	1
20R-1, 23	480.83	7A	P	5.77	32.7	3	1.6	AR	30–40	AF	C	2
20R-1, 47	481.07	7A	P	12.78	–25.2	4	3.8		425–500	TH	A	1
20R-1, 71	481.31	7A	P	4.42	36.5	4	1.0	AR	40–60	AF	A	2
20R-1, 72	481.32	7A	P	8.34						AF	D	2
20R-1, 117	481.77	7A	P	5.15	43.4	3	0.6	AR	30–40	AF	C	2
21R-1, 60	490.08	7A	P	12.31	32.6	5	1.8		25–45	AF	A	2
21R-1, 104	491.24	7A	P	29.82	45.3	4	2.7		450–525	TH	A	2
21R-2, 14	491.70	7A	P	6.50	64.5	3	5.1		475–525	TH	A	3
21R-2, 30	491.86	7B	P	5.36	–61.6*	3	2.1	AR	45–60	AF	B	3
21R-2, 30	491.86	7B	P	3.47	15.5	4	3.8		370–500	TH	B	2
21R-2, 62	492.18	7B	P	1.77	18.00	4	2.9	AR	40–60	AF	C	2
21R-2, 99	492.55	7B	P	5.13						TH	D	
21R-2, 136	492.92	7B	P	3.15	49.1	3	0.9	AR	35–45	AF	A	2
21R-2, 138	492.94	7B	P	2.56	–21.6	4	6.6		460–540	TH	A	5
21R-3, 46	493.45	7B	P	5.51						AF	B	2
21R-3, 55	493.54	7B	P	3.34	56.1	4	1.1	AR	30–45	AF	B	3
21R-3, 118	494.17	7B	P	3.12	11.5	4	6.6		40–60	AF	B	2
21R-4, 3	494.52	7B	P	8.00	–16.6	3	7.2		450–500	TH	A	5
21R-4, 49	494.98	7B	P	5.05	60.5	4	1.3	AR	40–60	AF	A	3
21R-4, 71	495.20	7B	P	31.86	52.9	5	4.1		425–525	TH	A	3

Table T1 (continued). (Continued on next page.)

Core, section, interval (cm)	Depth (mbsf)	Unit	Unit type	NRM (A/m)	Inc. (°)	*N*	MAD	Sample type	Demagnetization			ChRM type
									Steps	Treatment	Quality	
22R-1, 23	495.63	7B	P	15.86	–32.6*	4	3.4		40–60	AF	A	2
22R-1, 53	495.93	7B	P	3.55	49.9	5	0.7		35–60	AF	A	2
22R-1, 96	496.36	7B	P	11.16				AR		AF	D	
22R-1, 107	496.47	7B	P	5.65				AR		AF	D	
22R-1, 131	496.71	7B	P	11.74	57.6	4	5.2		425–500	TH	B	2
22R-2, 5	496.88	7B	P	4.60	58.4	5	0.7	AR	35–60	AF	A	3
22R-2, 26	497.09	7B	P	10.10	64.1	3	9.7		475–525	TH	A	3
22R-2, 48	497.31	7B	P	11.16	12.7	4	1.0	AR	30–45	AF	A	2
22R-2, 60	497.43	7B	P	7.95	50.8	5	2.0		30–50	AF	A	3
23R-1, 28	500.18	7B	P	10.81	50.8	5	2.2		380–540	TH	A	3
23R-1, 29	500.19	7B	P	7.11	46.9	4	1.9	AR	40–60	AF	A	2
23R-1, 50	500.40	7B	P	2.70	–31.5	5	14.1		425–525	TH	A	1
23R-1, 66	500.56	7B	P	4.81	37.6	3	1.1	AR	45–60	AF	B	2
23R-1, 93	500.83	7B	P	4.48						TH		
23R-1, 131	501.20	7B	P	5.81	50.4	4	2.5	AR	40–60	AF	B	3
23R-2, 10	501.46	7B	P	10.47						AF	C	
23R-2, 30	501.66	7B	P	3.56	46.5	4	8.4		460–540	TH	A	2
23R-2, 46	501.82	7B	P	5.62	50.6	3	4.3	AR	45–60	AF	B	3
23R-2, 89	502.25	7B	P	4.61	–18.8	4	3.2		460–540	TH	A	1
23R-2, 141	502.77	7B	P	7.64						AF	C	
23R-3, 8	502.94	7B	P	17.42	58.5	4	2.9		425–500	TH	A	3
23R-3, 24	503.10	7B	P	8.47	32.5	4	1.1	AR	30–45	AF	B	2
24R-1, 10	506.00	7B	P	3.68	–23.2	3	3.9		400–500	TH	B	5
24R-1, 13	506.03	7B	P	3.72	9.9	4	0.6	AR	35–50	AF	B	2
24R-1, 34	506.24	7B	P	7.14	–11.8	6	11.1		375–525	TH	C	1
24R-1, 55	506.45	7B	P	3.61	23.3	4	7.3		460–540	TH	A	5
24R-1, 59	506.49	7B	P	3.73	22.0	3	1.0	AR	35–45	AF	C	2
24R-1, 89	506.79	7B	P	5.19	32.0	4	2.4	AR	35–50	AF	C	2
24R-1, 103	506.93	7B	P	10.73	53.1	4	1.1	AR	35–50	AF	A	3
24R-1, 126	507.16	7B	P	30.43	53.7	6	10.2		400–525	TH	A	3
24R-2, 8	507.30	7B	P	3.00	35.4	3	2.6	AR	35–45	AF	A	2
24R-2, 9	507.31	7B	P	32.91	51.1	4	17.6		400–500	TH	B	4
24R-2, 37	507.59	7B	P	32.83	41.6	3	2.3		475–525	TH	A	2
25R-1, 11	509.61	7B	P	5.80	66.6	4	0.7	AR	35–50	AF	B	3
25R-1, 42	509.92	7B	P	3.21	–51.9	4	0.9		25–40	AF	B	1
25R-1, 54	510.04	7B	P	8.14	61.0	3	11.4		475–525	TH	B	
25R-1, 75	510.25	7B	P	4.46	55.8	4	2.5	AR	35–50	AF	A	3
25R-1, 110	510.60	7B	P	4.46	52.8	3	1.3	AR	35–45	AF	C	3
25R-1, 132	510.82	7B	P	15.32	74.2	5	3.9		400–500	TH	A	3
25R-2, 6	510.97	7B	P	9.70	40.3	3	7.3		475–525	TH	A	2
25R-2, 55	511.46	7B	P	3.90	43.6	3	1.5	AR	35–45	AF	B	2
25R-2, 76	511.67	7B	P	6.08	50.9	3	0.8	AR	35–45	AF	C	3
25R-2, 97	511.88	7C	P	11.35	–5.5	3	0.9		35–45	AF	B	1
26R-1, 37	515.87	7C	P	4.36	–69.4	5	7.9		450–500	TH	A	5
26R-1, 37	515.87	7C	P	3.13	51.3	4	1.2	AR	20–40	AF	A	3
27R-1, 66	519.66	7C	P	4.49	66.8	4	0.6	AR	30–45	AF	A	3
27R-1, 68	519.68	7C	P	10.26						AF	C	
27R-1, 84	519.84	7C	P	15.91	54.1	3	1.5		475–525	TH	A	3
27R-1, 136	520.36	7C	P	6.75	–65.1*	4	0.9	AR	35–50	AF	B	3
27R-2, 4	520.54	7C	P	5.98	62.9	3	1.6	AR	35–45	AF	C	3
27R-2, 13	520.63	7C	P	6.12	69.0	3	0.5	AR	30–40	AF	A	3
27R-2, 26	520.76	7C	P	17.10	68.4	4	12.5		425–500	TH	A	3
28R-1, 19	528.79	7C	P	8.40						TH	C	
28R-1, 46	529.06	7C	P	16.31	44.2	3	5.9		475–525	TH	A	2
28R-1, 49	529.09	7C	P	6.33	66.3	3	0.7	AR	30–40	AF	C	3
30R-1, 47	535.67	7C	P	8.61	48.7	4	2.3	AR	40–60	AF	B	2
30R-1, 63	535.83	7C	P	4.66	63.2	3	19.1		500–550	TH	C	3
30R-1, 98	536.18	7C	P	5.35	47.6	4	0.7	AR	35–50	AF	A	2
30R-1, 99	536.19	7C	P	4.22	–61.0	3	0.9		450–525	TH	A	5
30R-1, 106	536.26	7C	P	3.13	–46.2	3	5.1		500–550	TH	A	5
30R-1, 116	536.36	7C	P	7.59	–54.7	3	2.3	AR	45–60	AF	A	1
31R-1, 49	544.89	7C	P	3.18	52.9	3	7.2	AR	45–60	AF	C	3
31R-1, 51	544.91	7C	P	3.37	–43.7	3	9.2		500–550	TH	A	1
32R-1, 19	550.19	7C	P	2.64	–8.3	4	1.4	AR	30–45	AF	B	1
32R-1, 36	550.36	7C	P	11.36	21.8	4	3.9		40–60	AF	A	2
32R-1, 81	550.81	7C	P	4.99	39.9	3	2.4		475–550	TH	A	2
32R-1, 119	551.19	7C	P	3.66	55.4	3	3.2	PP	20–30	AF	C	4
32R-1, 129	551.29	7C	P	18.58	22.0	3	0.6	AR	35–45	AF	C	2
32R-2, 18	551.62	7C	P	5.28						AF	C	

Table T1 (continued).

Core, section, interval (cm)	Depth (mbsf)	Unit	Unit type	NRM (A/m)	Inc. (°)	*N*	MAD	Sample type	Demagnetization			ChRM type
									Steps	Treatment	Quality	
32R-2, 54	551.98	7C	P	5.84	55.8	3	0.2	AR	40–50	AF	B	3
32R-2, 83	552.27	7C	P	15.50	–30.2	3	1.9	AR	40–50	AF	B	1
32R-2, 105	552.49	7C	P	8.71	60.0	3	43.1		500–550	TH	B	3
32R-3, 4	552.98	7C	P	10.71	–13.0	3	14.8		450–525	TH	C	1
32R-3, 19	553.13	7C	P	5.09	–2.5	4	2.1	AR	35–50	AF	B	1
32R-3, 33	553.27	7C	P	7.23	–2.9	3	10.9		500–550	TH	A	1
33R-1, 67	554.67	7C	P	2.40	64.0	3	7.4		500–550	TH	A	3
33R-1, 83	554.83	7C	P	6.41	58.9	3	0.6	AR	30–40	AF	B	
33R-1, 110	555.10	7C	P	15.56						AF	C	
33R-1, 132	555.32	7C	P	3.53	43.4	4	1.7	AR	30–45	AF	B	2
33R-2, 7	555.57	7C	P	5.64	34.9	3	1.2	AR	40–50	AF	A	2
33R-2, 19	555.69	7C	P	6.16	–36.1	4	9.7		475–550	TH	A	1
33R-2, 40	555.90	7C	P	2.17	78.5	3	1.4	AR	30–40	AF	C	3
33R-2, 105	556.55	7C	P	3.11	37.7	4	1.6	AR	40–60	AF	B	2
33R-2, 124	556.74	7C	P	5.44	23.5	3	1.5		500–550	TH	A	2
34R-1, 3	560.63	7C	P	6.33	36.6	5	14.2		425–550	TH	A	2
34R-1, 28	560.88	7C	P	7.96	–38.8	4	1.1	AR	35–50	AF	C	1
34R-1, 49	561.09	7C	P	3.95	32.7	3	12.6		500–550	TH	A	2
34R-1, 80	561.40	7C	P	4.57	11.1	3	0.7	AR	35–45	AF	B	2
34R-2, 26	562.36	7C	P	4.16	–46.5	4	4.5		450–525	TH	A	1
34R-2, 35	562.45	7C	P	4.44	51.2	3	0.9	AR	40–50	AF	B	3
34R-2, 87	562.97	7C	P	4.64	–72.5	3	1.5	AR	35–45	AF	A	1
34R-2, 90	563.00	7C	P	13.15	–65.4	3	3.7		500–540	TH	B	3
34R-2, 98	563.08	7C	P	7.85	–46.3	4	2.3	AR	30–45	AF	A	3
34R-2, 119	563.29	7C	P	9.10	11.5	4	5.3		475–550	TH	B	2
35R-1, 16	563.76	7C	P	3.05	–0.6	4	4.3		475–550	TH	B	1
35R-1, 27	563.87	7C	P	7.61	–14.2	4	14.2		450–525	TH	A	4
35R-1, 54	564.14	7C	P	3.17				AR		AF		
35R-1, 72	564.32	7C	P	1.88	–28.2	5	2.8		350–500	TH	A	5
35R-1, 77	564.37	7C	P	7.17	45.2	3	1.3	AR	40–50	AF	A	2
35R-2, 20	565.27	8A	B	6.03	51.2	3	1.2	AR	35–45	AF	C	3
35R-2, 41	565.48	8A	B	5.07	38.2	4	1.3	AR	35–50	AF	A	2
35R-2, 96	566.03	8B	P	6.04	40.4	6	4.6		300–450	TH	A	2
35R-2, 104	566.11	8B	P	27.67	64.2	4	17.9		450–550	TH	A	3
35R-2, 118	566.25	8B	P	10.46	38.8	3	18.4		475–525	TH	A	2
35R-2, 128	566.35	8B	P	5.30	34.9	4	2.2	AR	40–60	AF	A	2
35R-2, 130	566.37	8B	P	44.43	48.70	12.1	3		245–270	TH	B	2
35R-3, 12	556.61	8B	P	21.16	32.1	4	17.5		450–525	TH	A	2
36R-1, 12	573.32	8C	P	3.25	–40.0	3	1.7		460–540	TH	A	5
36R-1, 30	573.50	8C	P	16.51	66.5	4	2.3	AR	40–60	AF	C	3
36R-1, 41	573.61	8C	P	7.00	34.6	3	2.7	AR	35–45	AF	C	2
36R-1, 90	574.10	8C	P	3.26	–52.6	5	6.3		450–550	TH	A	1
36R-1, 124	574.44	8C	P	5.74	56.4	3	0.7	AR	35–45	AF	B	3
36R-1, 144	574.64	8C	P	6.09	–19.9	2	7.5		525–550	TH	C	5
36R-2, 8	574.78	8C	P	4.25	–50.9	3	1.4		500–550	TH	A	5
36R-2, 85	575.55	8C	P	5.43	52.8	3	2.2	AR	35–45	AF	B	3
36R-2, 101	575.71	8C	P	8.19	53.9	3	1.7	AR	25–35	AF	C	3
36R-2, 122	575.92	8C	P	6.63	–55.3	4	3.3		475–550	TH	A	5
36R-3, 36	576.53	8C	P	3.76	–61.9	3	0.9		500–550	TH	A	1
36R-3, 85	577.02	8C	P	3.10	–25.1	4	9.6		450–550	TH	A	1

Notes: See the **"Site U1301"** chapter for igneous unit definitions. NRM = natural remanent magnetization, Inc. = inclination, *N* = number of measurements used for PCA analysis, MAD = maximum angle of deflection (a measure of the error in PCA analysis), Demagnetization quality = subjective judgement of demagnetization curve consistency ranging from A = excellent, simple isovectorial decay, to C = poor, poor consistency, small number of consistent steps, or departure from isovectorial decay, ChRM type = subjective classification of characteristic remanent magnetization direction. P = pillow basalt, M = massive flow. AR = archive-half sample, PP = physical properties sample. AF = alternating field, TH = thermal. * = thought to be inverted samples. † = ChRM inclinations calculated using a PCA solution anchored to the origin.

Table T2. Basalt sample IRM acquisition data, Hole U1301B. (See table notes.) (Continued on next page.)

Core, section, interval (cm):	Hole U1301B															
	7R-1, 12		7R-1, 12		15R-1, 44		15R-1, 44		15R-2, 141		15R-2, 141		15R-4, 135		15R-4, 135	
Step	Field (Oe)	Halo *M* (emu)	Field (Oe)	Normal *M* (emu)	Field (Oe)	Halo *M* (emu)	Field (Oe)	Normal *M* (emu)	Field (Oe)	Halo *M* (emu)	Field (Oe)	Normal *M* (emu)	Field (Oe)	Halo *M* (emu)	Field (Oe)	Normal *M* (emu)
1	0.8	2.08E–04	0.9	6.68E–05	0.9	1.34E–04	0.9	3.59E–04	0.9	1.45E–04	0.8	5.33E–05	0.9	1.82E–04	0.9	8.17E–05
2	128.0	1.99E–03	128.0	6.78E–04	128.1	4.44E–03	128.0	1.18E–02	250.4	1.04E–02	250.5	3.37E–03	128.0	1.65E–03	128.1	9.10E–04
3	250.3	1.10E–02	250.5	3.06E–03	250.5	8.80E–03	250.4	1.88E–02	500.1	1.90E–02	500.1	6.29E–03	250.5	9.87E–03	250.5	4.45E–03
4	377.5	1.96E–02	377.5	4.36E–03	377.6	1.06E–02	377.7	2.10E–02	754.5	2.16E–02	754.5	7.05E–03	377.7	1.79E–02	377.7	7.20E–03
5	499.9	2.40E–02	499.9	4.78E–03	500.0	1.14E–02	500.0	2.18E–02	1,003.6	2.26E–02	1,003.7	7.30E–03	500.0	2.25E–02	500.1	8.59E–03
6	626.9	2.60E–02	626.9	4.95E–03	627.0	1.18E–02	627.0	2.22E–02	1,253.0	2.31E–02	1,253.0	7.42E–03	627.0	2.52E–02	627.1	9.35E–03
7	754.4	2.71E–02	754.4	5.04E–03	754.2	1.20E–02	754.4	2.25E–02	1,502.4	2.33E–02	1,502.3	7.47E–03	754.4	2.68E–02	754.5	9.77E–03
8	876.1	2.76E–02	876.2	5.09E–03	876.1	1.21E–02	876.2	2.26E–02	1,751.9	2.35E–02	1,751.8	7.50E–03	876.2	2.77E–02	876.4	9.99E–03
9	1,003.4	2.79E–02	1,003.4	5.12E–03	1,003.4	1.22E–02	1,003.5	2.27E–02	2,001.1	2.36E–02	2,001.1	7.52E–03	1,003.5	2.83E–02	1,003.7	1.01E–02
10	1,125.7	2.80E–02	1,125.8	5.14E–03	1,125.7	1.23E–02	1,125.8	2.28E–02	2,255.5	2.37E–02	2,255.5	7.54E–03	1,125.9	2.88E–02	1,126.0	1.02E–02
11	1,252.6	2.82E–02	1,252.7	5.15E–03	1,252.6	1.23E–02	1,252.7	2.29E–02	2,504.4	2.37E–02	2,504.2	7.55E–03	1,252.8	2.91E–02	1,253.0	1.03E–02
12	1,374.9	2.82E–02	1,374.9	5.16E–03	1,374.9	1.23E–02	1,374.9	2.29E–02	2,753.8	2.37E–02	2,753.6	7.55E–03	1,375.0	2.93E–02	1,375.2	1.03E–02
13	1,502.0	2.83E–02	1,502.1	5.16E–03	1,502.0	1.24E–02	1,502.1	2.29E–02	3,003.1	2.38E–02	3,002.9	7.55E–03	1,502.2	2.94E–02	1,502.4	1.04E–02
14	1,629.1	2.83E–02	1,629.2	5.17E–03	1,629.2	1.24E–02	1,629.2	2.30E–02	3,252.3	2.38E–02	3,252.1	7.55E–03	1,629.4	2.96E–02	1,629.6	1.04E–02
15	1,751.3	2.84E–02	1,751.5	5.18E–03	1,751.2	1.24E–02	1,751.4	2.30E–02	3,501.7	2.38E–02	3,501.4	7.55E–03	1,751.7	2.96E–02	1,751.8	1.04E–02
16	1,878.3	2.84E–02	1,878.5	5.18E–03	1,878.4	1.24E–02	1,878.5	2.30E–02	3,755.6	2.38E–02	3,755.3	7.56E–03	1,878.6	2.97E–02	1,878.8	1.04E–02
17	2,000.5	2.84E–02	2,000.7	5.18E–03	2,000.6	1.24E–02	2,000.7	2.30E–02	4,004.7	2.38E–02	4,004.5	7.56E–03	2,000.9	2.98E–02	2,001.0	1.05E–02
18	2,127.7	2.84E–02	2,128.0	5.18E–03	2,127.8	1.24E–02	2,127.9	2.31E–02	4,254.4	2.38E–02	4,254.2	7.56E–03	2,128.1	2.98E–02	2,128.3	1.05E–02
19	2,254.9	2.84E–02	2,255.0	5.19E–03	2,254.9	1.24E–02	2,255.0	2.31E–02	4,503.4	2.38E–02	4,503.1	7.56E–03	2,255.2	2.99E–02	2,255.4	1.05E–02
20	2,377.1	2.85E–02	2,377.3	5.19E–03	2,377.1	1.24E–02	2,377.2	2.31E–02	4,752.7	2.38E–02	4,752.4	7.56E–03	2,377.4	2.99E–02	2,377.7	1.05E–02
21	2,503.6	2.85E–02	2,503.7	5.19E–03	2,503.6	1.24E–02	2,503.7	2.31E–02	5,001.6	2.38E–02	5,001.3	7.57E–03	2,504.0	2.99E–02	2,504.2	1.05E–02
22	2,626.0	2.85E–02	2,626.2	5.19E–03	2,626.0	1.24E–02	2,626.2	2.31E–02	5,255.5	2.38E–02	5,255.2	7.57E–03	2,626.3	3.00E–02	2,626.6	1.05E–02
23	2,752.9	2.85E–02	2,753.0	5.20E–03	2,752.8	1.24E–02	2,753.1	2.31E–02	5504.8	2.38E–02	5,504.4	7.57E–03	2,753.2	3.00E–02	2,753.6	1.05E–02
24	2,880.0	2.85E–02	2,880.2	5.20E–03	2,880.0	1.25E–02	2,880.2	2.31E–02	5,753.8	2.38E–02	5,753.4	7.57E–03	2,880.4	3.00E–02	2,880.6	1.05E–02
25	3,002.3	2.85E–02	3,002.3	5.20E–03	3,002.3	1.25E–02	3,002.5	2.31E–02	6,003.0	2.38E–02	6,002.6	7.57E–03	3,002.7	3.00E–02	3,002.9	1.05E–02
26	3,129.3	2.85E–02	3,129.4	5.21E–03	3,129.2	1.25E–02	3,129.5	2.32E–02	6,252.3	2.38E–02	6,251.9	7.58E–03	3,129.8	3.00E–02	3,130.0	1.05E–02
27	3,251.4	2.85E–02	3,251.4	5.21E–03	3,251.3	1.25E–02	3,251.4	2.32E–02	6,506.3	2.38E–02	6,505.9	7.57E–03	3,251.7	3.00E–02	3,252.1	1.05E–02
28	3,378.5	2.85E–02	3,378.5	5.21E–03	3,378.4	1.25E–02	3,378.5	2.32E–02	6,755.5	2.39E–02	6,755.0	7.57E–03	3,378.9	3.01E–02	3,379.2	1.05E–02
29	3,500.6	2.85E–02	3,500.6	5.21E–03	3,500.5	1.25E–02	3,500.7	2.32E–02	7,004.3	2.38E–02	7,003.8	7.57E–03	3,501.1	3.01E–02	3,501.4	1.05E–02
30	3,627.6	2.85E–02	3,627.7	5.21E–03	3,627.6	1.25E–02	3,627.7	2.32E–02	7,253.6	2.38E–02	7,253.1	7.58E–03	3,628.1	3.01E–02	3,628.4	1.05E–02
31	3,754.5	2.85E–02	3,754.5	5.21E–03	3,754.5	1.25E–02	3,754.6	2.31E–02	7,502.4	2.38E–02	7,501.9	7.57E–03	3,754.9	3.01E–02	3,755.3	1.05E–02
32	3,876.7	2.85E–02	3,876.7	5.21E–03	3,876.6	1.25E–02	3,876.8	2.32E–02	7,751.1	2.39E–02	7,750.6	7.57E–03	3,877.2	3.01E–02	3,877.5	1.05E–02
33	4,003.5	2.85E–02	4,003.7	5.21E–03	4,003.6	1.25E–02	4,003.7	2.32E–02	8,005.1	2.38E–02	8,004.5	7.57E–03	4,004.1	3.01E–02	4,004.5	1.05E–02
34	4,126.3	2.85E–02	4,126.4	5.21E–03	4,126.3	1.25E–02	4,126.4	2.32E–02	8,254.1	2.38E–02	8,253.4	7.58E–03	4,126.9	3.01E–02	4,127.2	1.05E–02
35	4,253.1	2.85E–02	4,253.3	5.21E–03	4,253.1	1.25E–02	4,253.3	2.32E–02	8,503.1	2.39E–02	8,502.5	7.58E–03	4,253.8	3.01E–02	4,254.1	1.05E–02
36	4,380.0	2.85E–02	4,380.2	5.21E–03	4,380.1	1.25E–02	4,380.2	2.32E–02	8,751.9	2.39E–02	8,751.2	7.57E–03	4,380.7	3.01E–02	4,381.1	1.05E–02
37	4,502.0	2.85E–02	4,502.2	5.21E–03	4,502.1	1.25E–02	4,502.3	2.32E–02	9,000.9	2.39E–02	9,000.2	7.58E–03	4,502.7	3.01E–02	4,503.1	1.05E–02
38	4,629.1	2.85E–02	4,629.3	5.21E–03	4,629.1	1.25E–02	4,629.2	2.32E–02	9,250.0	2.38E–02	9,249.4	7.58E–03	4,629.7	3.01E–02	4,630.1	1.05E–02
39	4,751.3	2.85E–02	4,751.4	5.21E–03	4,751.3	1.25E–02	4,751.5	2.32E–02	9,503.6	2.39E–02	9,503.0	7.58E–03	4,751.9	3.01E–02	4,752.4	1.05E–02
40	4,878.3	2.85E–02	4,878.4	5.21E–03	4,878.3	1.25E–02	4,878.4	2.32E–02	9,752.8	2.39E–02	9,752.1	7.57E–03	4,878.9	3.01E–02	4,879.4	1.05E–02
41	5,004.8	2.85E–02	5,004.9	5.22E–03	5,004.8	1.25E–02	5,005.0	2.32E–02	10,001.6	2.38E–02	10,001.0	7.58E–03	5,005.5	3.01E–02	5,006.0	1.05E–02

Notes: Field = applied field, *M* = magnetization. Halo = samples from alteration halos, normal = samples from adjacent rock.

Table T2 (continued).

Core, section, interval (cm):	Hole U1301B															
	18R-1, 36		18R-1, 36		18R-4, 140		18R-4, 140		25R-2, 79		25R-2, 79		33R-2,138		33R-2,138	
Step	Field (Oe)	Halo *M* (emu)	Field (Oe)	Normal *M* (emu)	Field (Oe)	Halo *M* (emu)	Field (Oe)	Normal *M* (emu)	Field (Oe)	Halo *M* (emu)	Field (Oe)	Normal *M* (emu)	Field (Oe)	Halo *M* (emu)	Field (Oe)	Normal *M* (emu)
1	0.9	1.45E–04	8.81E–01	7.07E–05	0.8	1.83E–04	0.8	2.92E–04	0.2	1.58E–04	0.9	1.99E–04	8.45E–01	1.49E–04	8.35E–01	1.77E–04
2	250.5	1.06E–02	2.50E+02	3.37E–03	128.0	1.60E–03	128.0	3.44E–03	50.1	3.29E–04	128.0	5.56E–03	2.50E+02	9.80E–03	2.50E+02	1.08E–02
3	500.2	1.42E–02	5.00E+02	3.75E–03	250.4	1.01E–02	250.5	1.55E–02	100.0	1.29E–03	250.4	1.29E–02	5.00E+02	1.76E–02	5.00E+02	1.41E–02
4	754.5	1.50E–02	7.54E+02	3.84E–03	377.6	1.85E–02	377.6	2.36E–02	150.0	4.13E–03	377.5	1.53E–02	7.54E+02	1.97E–02	7.54E+02	1.46E–02
5	1,003.8	1.53E–02	1.00E+03	3.87E–03	500.0	2.29E–02	500.0	2.69E–02	199.9	8.21E–03	500.0	1.60E–02	1.00E+03	2.04E–02	1.00E+03	1.47E–02
6	1,253.3	1.54E–02	1.25E+03	3.88E–03	626.9	2.53E–02	626.9	2.85E–02	251.2	1.24E–02	626.9	1.62E–02	1.25E+03	2.07E–02	1.25E+03	1.48E–02
7	1,502.7	1.55E–02	1.50E+03	3.89E–03	754.3	2.66E–02	754.4	2.93E–02	301.1	1.58E–02	754.3	1.63E–02	1.50E+03	2.09E–02	1.50E+03	1.48E–02
8	1,752.1	1.55E–02	1.75E+03	3.90E–03	876.1	2.74E–02	876.2	2.97E–02	351.1	1.86E–02	876.1	1.64E–02	1.75E+03	2.10E–02	1.75E+03	1.49E–02
9	2,001.4	1.56E–02	2.00E+03	3.90E–03	1,003.4	2.79E–02	1,003.5	3.00E–02	400.9	2.07E–02	1,003.4	1.65E–02	2.00E+03	2.10E–02	2.00E+03	1.49E–02
10	2,255.8	1.56E–02	2.25E+03	3.91E–03	1,125.7	2.82E–02	1,125.8	3.02E–02	450.8	2.23E–02	1,125.8	1.65E–02	2.26E+03	2.11E–02	2.26E+03	1.49E–02
11	2,504.7	1.56E–02	2.50E+03	3.91E–03	1,252.7	2.84E–02	1,252.7	3.03E–02	500.6	2.35E–02	1,252.7	1.65E–02	2.50E+03	2.11E–02	2.50E+03	1.49E–02
12	2,754.2	1.56E–02	2.75E+03	3.92E–03	1,374.8	2.85E–02	1,374.9	3.04E–02	550.5	2.44E–02	1,374.9	1.65E–02	2.75E+03	2.11E–02	2.75E+03	1.49E–02
13	3,003.5	1.56E–02	3.00E+03	3.92E–03	1,501.9	2.86E–02	1,502.0	3.05E–02	600.5	2.51E–02	1,502.0	1.65E–02	3.00E+03	2.11E–02	3.00E+03	1.49E–02
14	3,252.6	1.56E–02	3.25E+03	3.92E–03	1,629.1	2.87E–02	1,629.3	3.05E–02	651.9	2.56E–02	1,629.2	1.66E–02	3.25E+03	2.11E–02	3.25E+03	1.49E–02
15	3,502.0	1.56E–02	3.50E+03	3.92E–03	1,751.3	2.88E–02	1,751.5	3.06E–02	701.8	2.61E–02	1,751.5	1.66E–02	3.50E+03	2.11E–02	3.50E+03	1.49E–02
16	3,756.1	1.56E–02	3.75E+03	3.93E–03	1,878.3	2.88E–02	1,878.6	3.06E–02	751.5	2.64E–02	1,878.4	1.66E–02	3.76E+03	2.11E–02	3.75E+03	1.49E–02
17	4,005.3	1.56E–02	4.00E+03	3.93E–03	2,000.5	2.88E–02	2,000.8	3.07E–02	801.5	2.67E–02	2,000.6	1.66E–02	4.00E+03	2.11E–02	4.00E+03	1.49E–02
18	4,254.9	1.56E–02	4.25E+03	3.93E–03	2,127.8	2.89E–02	2,128.0	3.07E–02	851.3	2.69E–02	2,127.8	1.66E–02	4.25E+03	2.11E–02	4.25E+03	1.49E–02
19	4,503.9	1.56E–02	4.50E+03	3.93E–03	2,254.9	2.89E–02	2,255.0	3.07E–02	901.2	2.70E–02	2,254.9	1.66E–02	4.50E+03	2.11E–02	4.50E+03	1.49E–02
20	4,753.5	1.56E–02	4.75E+03	3.93E–03	2,377.1	2.89E–02	2,377.3	3.07E–02	951.2	2.72E–02	2,377.1	1.66E–02	4.75E+03	2.12E–02	4.75E+03	1.49E–02
21	5,002.3	1.56E–02	5.00E+03	3.93E–03	2,503.6	2.89E–02	2,503.8	3.08E–02	1,001.0	2.73E–02	2,503.7	1.66E–02	5.00E+03	2.12E–02	5.00E+03	1.49E–02
22	5,256.1	1.56E–02	5.25E+03	3.93E–03	2,626.1	2.90E–02	2,626.2	3.08E–02	1,050.9	2.74E–02	2,626.1	1.67E–02	5.25E+03	2.12E–02	5.25E+03	1.49E–02
23	5,505.5	1.56E–02	5.50E+03	3.93E–03	2,752.9	2.90E–02	2,753.1	3.08E–02	1,102.2	2.75E–02	2,752.9	1.67E–02	5.50E+03	2.12E–02	5.50E+03	1.49E–02
24	5,754.4	1.56E–02	5.75E+03	3.92E–03	2,880.0	2.90E–02	2,880.2	3.08E–02	1,152.1	2.76E–02	2,880.1	1.67E–02	5.75E+03	2.12E–02	5.75E+03	1.49E–02
25	6,003.8	1.56E–02	6.00E+03	3.92E–03	3,002.2	2.90E–02	3,002.4	3.08E–02	1,201.9	2.76E–02	3,002.3	1.67E–02	6.00E+03	2.12E–02	6.00E+03	1.49E–02
26	6,253.1	1.56E–02	6.25E+03	3.92E–03	3,129.2	2.90E–02	3,129.5	3.08E–02	1,251.9	2.77E–02	3,129.3	1.67E–02	6.25E+03	2.12E–02	6.25E+03	1.49E–02
27	6,507.0	1.56E–02	6.50E+03	3.92E–03	3,251.3	2.90E–02	3,251.6	3.09E–02	1,301.8	2.77E–02	3,251.4	1.67E–02	6.51E+03	2.12E–02	6.51E+03	1.49E–02
28	6,756.2	1.56E–02	6.75E+03	3.92E–03	3,378.4	2.90E–02	3,378.6	3.09E–02	1,351.6	2.78E–02	3,378.5	1.67E–02	6.75E+03	2.12E–02	6.75E+03	1.49E–02
29	7,005.1	1.56E–02	7.00E+03	3.92E–03	3,500.5	2.90E–02	3,500.8	3.09E–02	1,401.5	2.78E–02	3,500.7	1.67E–02	7.00E+03	2.12E–02	7.00E+03	1.49E–02
30	7,254.5	1.56E–02	7.25E+03	3.92E–03	3,627.5	2.90E–02	3,627.8	3.09E–02	1,451.4	2.78E–02	3,627.7	1.67E–02	7.25E+03	2.11E–02	7.25E+03	1.49E–02
31	7,503.3	1.56E–02	7.50E+03	3.92E–03	3,754.4	2.90E–02	3,754.7	3.09E–02	1,501.2	2.79E–02	3,754.6	1.67E–02	7.50E+03	2.11E–02	7.50E+03	1.49E–02
32	7,752.0	1.56E–02	7.75E+03	3.92E–03	3,876.5	2.90E–02	3,876.9	3.09E–02	1,552.6	2.79E–02	3,876.7	1.67E–02	7.75E+03	2.11E–02	7.75E+03	1.49E–02
33	8,006.0	1.56E–02	8.00E+03	3.92E–03	4,003.5	2.90E–02	4,003.8	3.09E–02	1,602.4	2.79E–02	4,003.7	1.67E–02	8.00E+03	2.11E–02	8.00E+03	1.49E–02
34	8,255.0	1.56E–02	8.25E+03	3.92E–03	4,126.2	2.90E–02	4,126.6	3.09E–02	1,652.3	2.79E–02	4,126.5	1.67E–02	8.25E+03	2.11E–02	8.25E+03	1.49E–02
35	8,504.0	1.56E–02	8.50E+03	3.92E–03	4,253.1	2.90E–02	4,253.5	3.09E–02	1,702.2	2.79E–02	4,253.3	1.67E–02	8.50E+03	2.11E–02	8.50E+03	1.49E–02
36	8,753.1	1.56E–02	8.75E+03	3.92E–03	4,380.0	2.90E–02	4,380.4	3.09E–02	1,752.0	2.80E–02	4,380.2	1.67E–02	8.75E+03	2.11E–02	8.75E+03	1.49E–02
37	9,002.0	1.56E–02	9.00E+03	3.91E–03	4,502.0	2.91E–02	4,502.4	3.09E–02	1,801.9	2.80E–02	4,502.2	1.67E–02	9.00E+03	2.11E–02	9.00E+03	1.49E–02
38	9,251.1	1.56E–02	9.25E+03	3.92E–03	4,629.0	2.91E–02	4,629.4	3.09E–02	1,851.9	2.80E–02	4,629.3	1.67E–02	9.25E+03	2.11E–02	9.25E+03	1.49E–02
39	9,504.8	1.56E–02	9.50E+03	3.92E–03	4,751.2	2.91E–02	4,751.6	3.09E–02	1,901.7	2.80E–02	4,751.5	1.67E–02	9.50E+03	2.11E–02	9.50E+03	1.49E–02
40	9,754.0	1.56E–02	9.75E+03	3.92E–03	4,878.3	2.91E–02	4,878.6	3.09E–02	1,953.0	2.80E–02	4,878.5	1.67E–02	9.75E+03	2.11E–02	9.75E+03	1.49E–02
41	10,002.9	1.56E–02	1.00E+04	3.92E–03	5,004.8	2.91E–02	5,005.1	3.09E–02	2,002.8	2.80E–02	5,005.0	1.67E–02	1.00E+04	2.11E–02	1.00E+04	1.49E–02

Table T3. Basalt sample hysteresis parameters, Hole U1301B. (See table notes.)

Core, section, interval (cm)	Depth (mbsf)	M_r	M_s	M_r/M_s	H_c	H_{cr}	H_{cr}/H_c	NRM	T_c
301-U1301B-									
2R-1, 100	358.10	3.103	10.500	0.294	110.50	151.80	1.374	4.055	339
4R-1, 51	367.11	9.201	27.370	0.336	139.80	193.20	1.382	7.967	359
5R-1, 100	377.30	5.270	17.220	0.306	90.53	128.40	1.418	4.358	349
6R-2, 48	387.93	2.226	7.382	0.302	108.50	156.90	1.446	4.054	339
12R-1, 70	429.60	1.911	11.570	0.165	42.15	90.47	2.146	15.500	128
13R-1, 45	430.35	5.157	31.210	0.165	35.85	66.97	1.868	48.280	149
13R-1, 120	431.10	2.360	8.820	0.215	64.20	94.83	1.477	0.434	179
15R-2, 70	445.80	3.210	16.400	0.196	65.71	122.60	1.866	0.445	128
15R-2, 78	445.88	2.693	12.800	0.210	67.43	137.80	2.044	27.130	159
15R-2, 127	446.37	4.230	15.500	0.272	72.80	99.81	1.371	0.446	289
15R-3, 24	446.84	2.500	12.620	0.198	67.86	108.20	1.594	42.100	219
15R-3, 120	447.80	2.758	12.240	0.225	59.14	90.59	1.532	41.453	260
15R-4, 30	448.4	4.307	20.480	0.210	53.99	82.78	1.533	16.771	370
15R-4, 115	449.25	3.022	13.370	0.226	65.18	121.30	1.861	58.429	190
18R-1, 55	471.55	4.071	12.570	0.324	103.60	150.40	1.452	6.583	339
18R-2, 50	472.80	1.782	15.280	0.117	36.42	81.63	2.241	19.308	129
18R-2, 102	473.32	1.370	13.400	0.102	35.09	74.00	2.109	12.552	149
18R-3, 25	473.81	1.638	13.510	0.121	35.33	74.40	2.106	35.066	129
18R-3, 58	474.14	1.046	15.260	0.069	43.97	61.69	1.403	23.534	128
18R-4, 112	476.00	2.930	6.656	0.441	190.40	257.10	1.350	1.522	339
21R-2, 30	491.86	2.890	6.478	0.446	159.30	207.50	1.303	2.774	369
21R-2, 138	492.94	3.007	9.997	0.301	107.60	153.90	1.430	2.047	349
23R-1, 28	500.18	3.275	10.390	0.315	108.30	159.70	1.475	8.647	339
23R-2, 30	501.66	4.630	14.560	0.317	125.30	173.00	1.381	2.847	334
23R-2, 89	502.25	6.003	15.620	0.384	166.80	215.90	1.294	3.686	349
24R-1, 10	506.00	4.949	10.090	0.491	203.60	259.30	1.274	2.941	359
24R-1, 55	506.45	2.302	5.155	0.447	170.70	222.70	1.305	3.601	359
34R-2, 90	563.00	3.086	14.100	0.219	71.02	113.20	1.594	10.519	349
35R-1, 72	564.32	4.518	12.540	0.360	129.10	178.90	1.386	1.507	365
35R-2, 96	566.03	3.290	11.000	0.325	110.00	158.00	1.440	1.507	364
35R-2, 130	566.37	3.285	10.110	0.325	110.00	158.90	1.445	4.829	359
36R-1, 12	573.32	3.977	9.824	0.405	162.50	221.60	1.364	2.602	369

Notes: M_r = saturation remanence, M_s = saturation magnetization. H_c = remanent coercive force, H_{cr} = ordinary coercive force. NRM = natural remanent magnetization. T_c = Curie temperature.

Table T4. Hysteresis measurements from halo/nonhalo paired samples, Hole U1301B. (See table notes.)

Core, section, interval (cm)	Type	M_s (emu)	M_r (emu)	H_c (Oe)	S*	H_{cr} (Oe)	H_{cr}/H_c	M_{rs}/M_s
301-U1301B-								
7R-1, 12	Halo	0.0654	0.0290	177.90	0.27	230.80	1.30	0.44
7R-1, 12	Normal	0.0161	0.0053	112.70	0.18	189.90	1.69	0.33
15R-1, 44	Halo	0.0419	0.0125	87.28	0.12	119.80	1.37	0.30
15R-1, 44	Normal	0.1003	0.0232	60.60	0.09	96.30	1.59	0.23
15R-2, 141	Halo	0.0646	0.0241	150.80	0.17	208.00	1.38	0.37
15R-2, 141	Normal	0.0206	0.0077	135.90	0.16	250.00	1.84	0.37
15R-4, 135	Halo	0.0596	0.0305	206.30	0.21	255.40	1.24	0.51
15R-4, 135	Normal	0.0213	0.0106	180.70	0.25	227.80	1.26	0.50
18R-1, 36	Halo	0.0435	0.0157	105.40	0.19	157.70	1.50	0.36
18R-1, 36	Normal	0.0223	0.0039	42.21	0.10	135.40	3.21	0.18
18R-4, 140	Halo	0.0581	0.0296	200.80	0.27	244.90	1.22	0.51
18R-4, 140	Normal	0.0727	0.0313	147.20	0.26	201.30	1.37	0.43
25R-2, 79	Halo	0.0706	0.0287	160.70	0.22	211.80	1.32	0.41
25R-2, 79	Normal	0.0542	0.0168	84.62	0.20	121.50	1.44	0.31
33R-2, 138	Halo	0.0584	0.0214	148.40	0.21	199.50	1.34	0.37
33R-2, 138	Normal	0.0506	0.0150	86.90	0.17	150.90	1.74	0.30

Notes: M_s = saturation magnetization, M_r = saturation remanence. H_c = remanent coercive force, H_{cr} = ordinary coercive force. S* = $2(H2/H_c) - 1$, where $H2$ is field value corresponding to 1/2 M_r.